frontiers | Frontiers in Materials

TYPE Review
PUBLISHED 02 September 2022
DOI 10.3389/fmats.2022.964992

OPEN ACCESS

EDITED BY
Lai-Chang Zhang,
Edith Cowan University, Australia

REVIEWED BY
Zhuoran Zeng,
Australian National University, Australia
Huan Liu,
Hohai University, China

*CORRESPONDENCE
Zhaoming Yan,
zmyan1027@nuc.edu.cn
Yong Xue,
yongxuenuc@126.com

SPECIALTY SECTION
This article was submitted to Structural Materials,
a section of the journal
Frontiers in Materials

RECEIVED 09 June 2022
ACCEPTED 26 July 2022
PUBLISHED 02 September 2022

CITATION
Yan Z, Zhu J, Zhang Z, Wang Q and Xue Y (2022), The microstructural, textural, and mechanical effects of high-pressure torsion processing on Mg alloys: A review.
Front. Mater. 9:964992.
doi: 10.3389/fmats.2022.964992

The microstructural, textural, and mechanical effects of high-pressure torsion processing on Mg alloys: A review

Zhaoming Yan[1,2]*, Jiaxuan Zhu[3], Zhimin Zhang[1,2,3], Qiang Wang[1,2] and Yong Xue[1,2]*

[1]School of Materials Science and Engineering, North University of China, Taiyuan, China, [2]Engineering Research Center for Magnesium-base Material Processing Technology, Ministry of Education, North University of China, Taiyuan, China, [3]College of Mechatronics Engineering, North University of China, Taiyuan, China

Magnesium (Mg) alloys attract considerable attention in the fields of aerospace, defense technology, and automobile production, owing to the advantages of their low density, their highly specific strength/stiffness, and their good damping and electromagnetic shielding performance. However, low strength and poor ductility limit further application. Severe plastic deformation is considered the most promising means of producing ultrafine-grained Mg alloys and improving their mechanical properties. To this end, high-pressure torsion (HPT) is one of the most effective techniques. This article outlines the microstructure, texture, and mechanical properties of Mg alloys processed using HPT. The effects of deformation parameters, such as processing temperature, turns, applied pressure, and rotation speed, on the grain refinement and secondary phases are discussed. Textural evolution is detailed in light of both intrinsic and extrinsic factors, such as cumulative strain and the composition of the alloy elements. The subsequent enhancement of mechanical properties and mechanisms, and the significant contribution of the HPT process to strength are further reviewed. Given the advantages of HPT for grain refinement and structural modification, researchers have proposed several novel processes to extend the industrial application of these alloys.

KEYWORDS

Mg alloys, high-pressure torsion, ultrafine grain size, texture, properties

1 Introduction

Mg and its alloys are the lightest metal structural materials, and possess various advantages (Zheng and Gu, 2011; Zhou et al., 2012; Fu et al., 2014; Chen et al., 2019; Meng et al., 2019; Wang et al., 2020; Yan et al., 2020; Xie et al., 2021; Jia et al., 2022; Li et al., 2022). To date, some Mg alloys have been used for aerospace and automotive components. However, with their hexagonal close-packed (HCP) structure, they have limited slip systems and ductility at room temperature (Liu et al., 2019). Their application has been considerably hampered by this poor ductility and formability. It is well

established, however, that a significant improvement in the microstructure and mechanical properties of Mg alloys can be achieved through plastic deformation (Wang et al., 2021; Heydarinia et al., 2022; Mansoor et al., 2022).

In recent years, many researchers have developed Mg alloys to produce excellent comprehensive performance by adjusting the processing technology (Gu et al., 2022; Ma et al., 2022; Shao et al., 2022). Traditional methods, such as forging, extrusion, and rolling, have been applied to producing the Mg alloy tubes, sheets, and strips. Now the processing of metals through severe plastic deformation (SPD) is attracting considerable interest, due to SDP's ability to create intense plastic strain without introducing changes to the dimensions of work pieces (Dong et al., 2021; Gunderov et al., 2021; Ren et al., 2021; Zhao et al., 2021; Roghani et al., 2022). Furthermore, a number of recent publications demonstrate that SPD techniques are capable of producing materials possessing ultrafine grain sizes within the submicrometer or nanometer range, as well as both high strength and ductility (Kasaeian-Naeini et al., 2021). Equal channel angular pressing (ECAP) (Valiev and Langdon, 2006; Abd El Aal, 2021), high-pressure torsion (HPT) (Zhilyaev and Langdon, 2008; Korneva, 2015), accumulative rolling bonding (ARB) (Saito et al., 1998; Hosseini and Manesh, 2009), and multidirectional forging (MDF) (Nie et al., 2011; Tang et al., 2013) have received the most scientific and industrial attention.

The ECAP process consists of a special die structure attached at a certain angle between the transverse channel and the longitudinal channel, and a round or square shape billet passing through the cross-channel to achieve the strong shear strain (Furukawa et al., 1998). Meanwhile, the billet size remains unchanged, which permits a repetition of the deformation and hence a large accumulation of strain. Moreover, different processing routes based on the rotation of the ECAPed billets, and changes of angle between channels, can also lead to evolution in various microstructural and mechanical properties. In ARB processing, thickness of the sheets is usually reduced by 50% by rolling. The ARBed sheets are cut in two, stacked together, and wire-brushed to achieve the original state (Saito et al., 1998; Verstraete et al., 2015). Consequently, several repetitions are possible to achieve large strains. MDF is a processing method that seems to have great potential for producing large-scale components that may be suitable for industrial applications. The billet is pressed along orthogonal directions, and repetition deformation with high accumulative strain is obtained. MDF has been applied to fabricate ultrafine-grained metallic materials, such as steels (Belyakov et al., 2000), Al alloys (Sitdikov et al., 2009), Ti alloys (Zherebtsov et al., 2004), and Mg alloys (Xing et al., 2008; Miura et al., 2011; Miura et al., 2012).

HPT is an attractive processing technique because there is good evidence demonstrating its significant grain refinement ability in bulk metal solids. The disc sample undergoes a shear strain under high hydrostatic pressure. Compared with other SPD processes, HPT does not only produce finer grain sizes

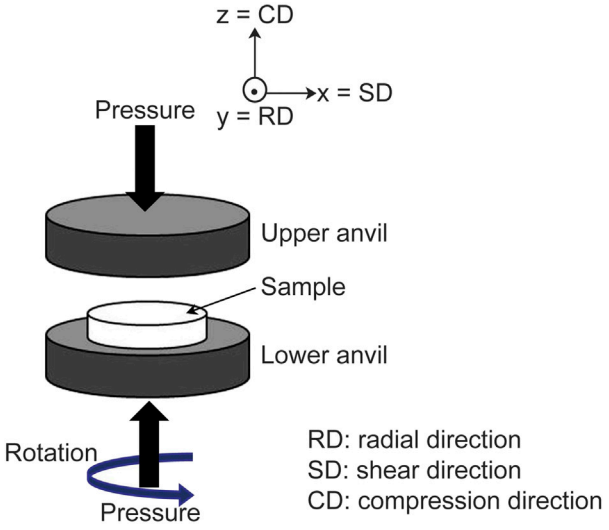

FIGURE 1
Schematic representation of HPT process (Azzeddine et al., 2022).

and a higher fraction of high-angle grain boundaries (Valiev et al., 1990; Valiev et al., 1991; Valiev et al., 1993; Wadsack et al., 2003; Valiev et al., 2006; Zhilyaev and Langdon, 2008; Borchers et al., 2015), but can also achieve many other features, such as enhanced atomic diffusion (Wilde et al., 2010), high density lattice defects (Wang et al., 2009; Ciuca et al., 2010; Oberdorfer et al., 2010; Cizek et al., 2011), high ductility (Valiev et al., 2002), superplasticity (Sergueeva et al., 2001), high electrical conductivity (Champion et al., 2010), and many other functional properties expected of nanocrystalline materials (Gleiter, 1989; Gleiter, 2000). However, the character of HPTed structures is closely related to the processing regimes and the initial microstructure of the original material. Meanwhile, microstructure refinement during HPT is typically accompanied by transformation of secondary phases, which makes the analysis of nanostructures more complicated, but increases their variety.

In this article, recent research studies into ultrafine-grained Mg alloys prepared by HPT are critically reviewed in terms of effect factors, while the texture evolution, deformation behavior, mechanical properties' enhancement, and strengthening mechanisms are more extensively detailed. In addition, novel SPD technologies based on the principles of HPT are also reviewed, and topics for further investigation are listed.

2 The principles of HPT

The scientific origin of modern HPT processing can be traced to a classic paper written by Percy Bridgman, whose ideas were concentrated on the effects of high pressure on solids (Bridgman,

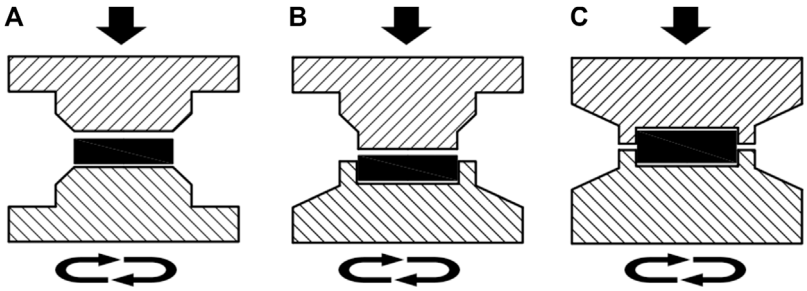

FIGURE 2
Schematical illustration of different conditions within the HPTed disk sample: **(A)** unconstrained; **(B,C)** constrained (Zhilyaev and Langdon, 2008).

1909a; Bridgman, 1909b; Bridgman, 1911a; Bridgman, 1911b; Bridgman, 1940; Bridgman, 1941). He was awarded the 1946 Nobel Prize in Physics for his contribution in the field of high-pressure physics. Subsequently, HPT has attracted more and more attention.

The principles of modern HPT processing are shown schematically in Figure 1 (Azzeddine et al., 2022). The whole process is a combination of compression and torsion. To be specific, the disk sample is located between two anvils, where it is subjected to a compressive pressure, P, of several GPa at ambient or elevated temperatures. Torsional strain, which is imposed by the rotation of the lower anvil, is applied simultaneously. The shear deformation therefore comes from the surface frictional forces, and the processing occurs under a quasi-hydrostatic pressure.

When a disk sample is processed by HPT, the equivalent von Mises strain, ε_{eq}, is given by the following equation (Valiev et al., 1996).

$$\varepsilon_{eq} = \frac{2\pi Nr}{\sqrt{3}h} \quad (1)$$

where N is the number of HPT turns, r and h are the radius and height (or thickness) of the disk sample. In practice, the preceding equations may be used to estimate the strains imposed on disks subjected to HPT. It can be noticed from Eq. 1 that the strain varies from zero at the center to the maximum at the periphery, which implies that the microstructure and hardness reveal an inevitable inhomogeneity within the HPTed disk sample. However, extensive experiments have revealed that a reasonable level of homogeneity of microstructure and hardness can be observed with the increase in HPT turns under application of high pressure (Xu et al., 2007; Cepeda-Jiménez et al., 2014; Bazzarnik et al., 2016; Zhang et al., 2021).

Figure 2 illustrates two different types of HPT molds found in the literature: constrained and unconstrained HPT (Zhilyaev and Langdon, 2008). In the unconstrained condition, as shown in Figure 2A, the material is free to flow outwards in a radial direction in a simple design, resulting in low hydrostatic pressure and significant sample thinning. In constrained HPT, a more homogeneous microstructure and greater hardness are obtained through the disk sample fitting into a cavity in the lower anvil. In Figure 2B, there is no outward flow of material during the torsional strain, which means effective back pressure is applied. However, it is difficult to perform experiments in an absolutely constrained condition, and the semi-constrained condition shown in Figure 2C is more common, where the height of the disk sample is greater than the depth of the lower anvil, and limited outward flow of material is achieved.

Thus far, HPT has been regarded not only as an SPD method in metallurgy, but also as an important scientific tool in many fields of science and engineering (Perez-Prado et al., 2008; Leiva et al., 2010; Nie et al., 2010; Gao et al., 2011; Mine et al., 2011; Popov et al., 2012a; Estrin and Vinogradov, 2013). HPT processing has been applied to many kinds of materials, such as metallic and intermetallic materials, and metal-based, polymer-based, and ceramic-based composites (Towle and Riecker, 1969; Shabashov, 1995; Huang, 2007; Hohenwarter and Pippan, 2011; Tugcu et al., 2012; Edalati et al., 2013; Kawasaki et al., 2014a; Langdon, 2015; Medvedev et al., 2018; Danilenko et al., 2021; Xiong et al., 2021). Compared with traditional thermomechanical processing methods, such as forging, extrusion, and rolling, HPT has the advantage of extensive cumulative strain, which can refine the microstructure to submicrometer or nanometer range. As illustrated by the Hall–Petch relation, the strength of a material is reversely proportional to its grain size, and the ultrafine-grained materials processed by HPT can achieve extremely high strength or superplasticity (Sergueeva et al., 2001). In comparison with other major SPD methods (Yang et al., 2008; Dheda and Mohamed, 2011; Zhen et al., 2021), such as ECAP, ARB, and MDF, HPT processing is more effective in grain refinement, and hence lower in manufacturing cost. Furthermore, the compression strain introduced by hydrostatic pressure, and the shear strain introduced by torsional deformation, creates sufficient deformation for various alloys. However, the small-scale

TABLE 1 Microstructural evolution of Mg alloys processed by HPT.

Material	Parameters	HPTed GS	Secondary phases	Ref
Pure Mg	5 turns, RT, 6.0 GPa, and 1 rpm	Lager size of 1.8 ± 0.5 μm and finer size of 590 ± 120 nm	—	Wenting Li et al. (2020)
Mg-1Ca	5 turns, RT, 6.0 GPa, and 1 rpm	171 ± 52 nm	Mg_2Ca: a diameter of 6 ± 2 μm	Wenting Li et al. (2020)
Mg-2Sr	5 turns, RT, 6.0 GPa, and 1 rpm	720 ± 180 nm	$Mg_{17}Sr_2$: 35 ± 6 μm and 10 ± 3 μm	Wenting Li et al. (2020)
Mg-3.4Zn	20 turns, RT, 5.0 GPa, and 1 rpm	140 ± 50 nm	$MgZn_2$: 10–20 nm	Meng et al. (2014)
Mg-9Li	10 turns, RT, 6.0 GPa, and 1 rpm	230 nm	Bcc β phases	Su et al. (2018)
Mg-0.41Dy	15 turns, RT, 6.0 GPa, and 1 rpm	0.7 ± 0.1 μm	—	Hanna et al. (2019a)
Mg-22Gd	15 turns, RT, and 2.0 GPa	300 nm	Nanoscale $Mg_{46}Gd_9$	Čížek et al. (2017)
Mg-3Al-1Zn	10 turns, RT, 6.0 GPa, and 1 rpm	110 nm	—	Xu et al. (2015)
Mg-6Al-1Zn	7 turns, (RT, 100, and 150°C), 3.0 GPa, and 1 rpm	0.11 μm at RT, 0.22 μm at 150 °C	—	Harai et al. (2008a)
Mg-9Al-1Zn	10 turns, (RT, 150, and 200°C), 3.0 GPa, and 1 rpm	35 nm at RT, 180 nm at 150°C, 250 nm at 200°C	β-phases: 200 nm	Al-Zubaydi et al. (2016)
Mg-1Mn-1Nd	5 turns, RT, and 6.0 GPa	200 nm	Nanometer Mg_3Nd	de Oliveira et al. (2021)
Mg-5.5Zn-0.5Zr	5 turns, RT, 2.0 GPa, and 1 rpm	700 nm	—	Torbati-Sarraf et al. (2018)
Mg-1Zn-0.13Ca	5 turns, RT, and 6.0 GPa	150 nm	$Ca_2Mg_6Zn_3$: 1 μm in length and 0.5 μm in thick; Mg_2Ca:10 nm	Kulyasova et al. (2015)
Mg-4.97Sm-0.84Ca	4 turns, RT, 5.0 GPa, and 1 rpm	70 nm	Nanoscale $Mg_{41}Sm_5$	Liu et al. (2020)
Mg-8.10Zn-5.08Y	7 turns, RT, 5.0 GPa, and 1 rpm	53 nm	Nanoscale $Mg_3Y_2Zn_3$	Li et al. (2020b)
Mg-6.2Zn-0.5Zr-0.2Ca	5 turns RT, 6.0 GPa, and 0.2 rpm	0.77 and 0.98 μm	Nanoscale and finely dispersed β' phases	Zheng et al. (2017)
Mg-8.2Gd-3.8Y-1.0Zn-0.4Zr	16 turns, RT, 6.0 GPa, and 1 rpm	55 nm	Mg_3(Gd, Y) and LPSO phases: 1–10 μm	Sun et al. (2017a)
Mg-3.56Y-2.20Nd-0.47Zr	10 turns, 20–300°C, 6.0 GPa, and 1 rpm	Twin size of 0.4–8.1 μm, fine structure with size of 30–100 nm	A small amount of $Mg_{41}Nd_5$ phases	Lukyanova et al. (2016)
Mg-8.03Al-0.5Zn-0.02Mn/SiC	10 turns, RT, 2.5 GPa, and 1 rpm	2.5 ± 2.1 μm	β-$Mg_{17}Al_{12}$ and nano SiC particles	Akbaripanah et al. (2021)

RT, room temperature; GS, grain size.

production, heterogeneous microstructure evolution, and high equipment requirements limit the further application of HPT processing. Thus, determining the influence factor of HPT processing, and understanding how to take maximum advantage of HPT are the main purposes of this review.

3 Effect of fundamental parameters on microstructural evolution

It is well known that grain size is an exceptionally important structural parameter in polycrystalline metals. During HPT processing, changing the deformation parameters, such as the processing temperature, turns, applied pressure, and rotation speed, can effectively impact microstructural evolution, especially grain refinement behavior (Harai et al., 2008a; Meng et al., 2014; Kulyasova et al., 2015; Xu et al., 2015; Al-Zubaydi et al., 2016; Lukyanova et al., 2016; Sun et al., 2017a; Zheng et al., 2017; Čížek et al., 2017; Su et al., 2018; Torbati-Sarraf et al., 2018; Hanna et al., 2019a; Li W. T. et al., 2020; Li Y. S. et al., 2020; Liu et al., 2020; Akbaripanah et al., 2021; de Oliveira et al., 2021). Table 1 summarizes the influence of deformation parameters on the microstructural evolution of Mg alloys processed by HPT. It can be seen that the grain sizes and secondary phases of pure Mg, traditional commercial Mg alloys, and Mg alloys containing rare-earth elements, are significantly refined to submicrometer or nanometer range. An obviously heterogeneous structure can also be observed due to the character of the torsion process, in which a higher strain is concentrated on the edge of the workpiece, rather than in the center. Moreover, the finer grain sizes and secondary phases of HPTed alloys are easily obtained at low deformation temperatures, and with high numbers of rotations.

3.1 Processing temperature

Processing temperature is an important factor affecting the plastic deformation process. According to thermodynamic

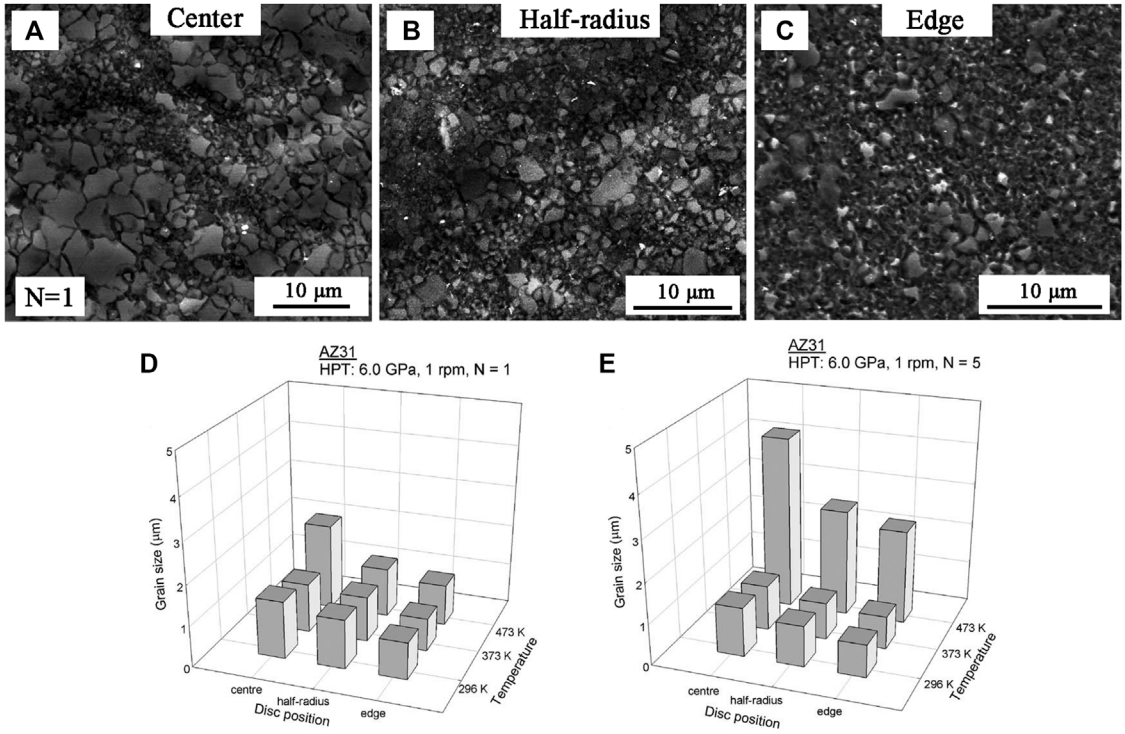

FIGURE 3
The grain refinement of HPTed AZ31 alloys at **(A)** the center, **(B)** the half-radius, **(C)** the edge position, and the grain size distribution of different temperatures through **(D)** 1 turn and **(E)** 5 turns (Huang et al., 2012).

theory, the internal energy of the atom increases with an increasing temperature, and dislocation activity is enhanced, especially for Mg alloys with low stacking fault energies. Dynamic recovery and dynamic recrystallization achieve grain refinement with an increasing temperature that falls within a certain temperature range, although coarsening happens when this range is exceeded, and cracking occurs below it (Edalati et al., 2011; Huang et al., 2012; Dobatkin et al., 2016; Alsubaie et al., 2017; Ji et al., 2021; Xu et al., 2022; Zhao et al., 2022).

Figure 3 shows the investigative results of Huang et al. (2012), who evaluated the strength and microstructural homogeneity of AZ31 alloys processed by HPT at room temperature, 100, and 200°C. It can be observed that the submicrometer range of grain sizes was observed at room temperature and 100°C through 5 turns, and a saturation in Vickers microhardness at high strains with a hardness value of 105 HV. Processing by HPT at 200°C led to obvious grain growth and decreased microhardness. Dobatkin et al. (2016) studied the influence of deformation temperature on the structure and mechanical properties of Mg-Y-Gd-Zr during HPT, and the results showed that grain size reached 20–30 nm at room temperature and increased to 60–90 nm at 200°C. Moreover, at 250°C the HPTed alloy had substantial strengthening and thermal stability. According to the report of Alsubaie et al. (2017), the microstructural homogeneity of AZ80 alloys processed by HPT improved with increasing deformation turns. The research into microhardness evolution at ambient and elevated temperatures showed that grain growth at 200°C resulted in lower microhardness values. The precipitates played an important part in achieving high microhardness at the elevated temperature.

3.2 Turns

According to Equation 1, equivalent strain in the HPT process is mainly determined by turns. Many studies prove that the submicron or nanosized grains can be observed when increasing turns (Harai et al., 2008a; Edalati et al., 2011; Huang et al., 2012; Meng et al., 2014; Alhamidi and Horita, 2015; Kulyasova et al., 2015; Xu et al., 2015; Al-Zubaydi et al., 2016; Alsubaie et al., 2016; Dobatkin et al., 2016; Lukyanova et al., 2016; Alsubaie et al., 2017; Sun et al., 2017a; Jahedi et al., 2017; Zheng et al., 2017; Čížek et al., 2017; Gu et al., 2018; Su et al., 2018; Torbati-Sarraf et al., 2018; Hanna et al., 2019a; Yang et al., 2019; Li W. T. et al., 2020; Bednarczyk et al., 2020; Li Y. S. et al., 2020;

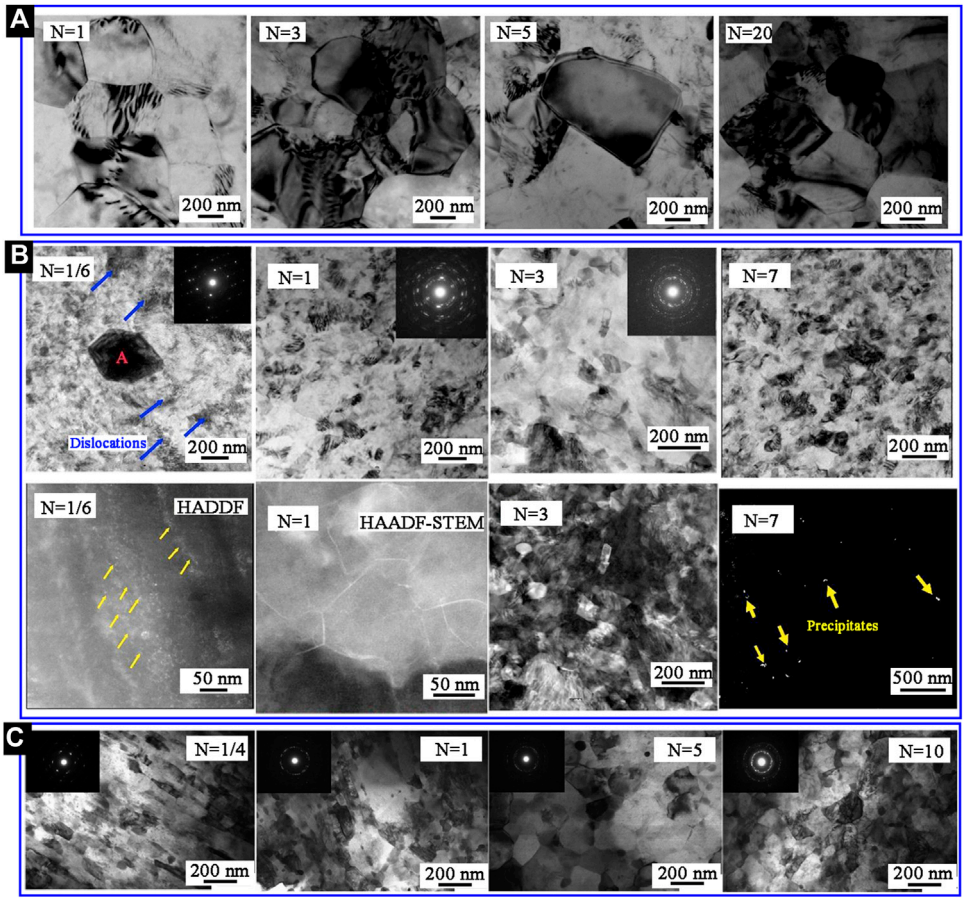

FIGURE 4
Ultrafine-grained structures processed by HPT process for **(A)** pure Mg (Gu et al., 2018), **(B)** AZ31 alloys (Li Y. S. et al., 2020), and **(C)** AZ80 alloys (Alsubaie et al., 2016) through different revolutions.

Kong et al., 2020; Liu et al., 2020; Akbaripanah et al., 2021; de Oliveira et al., 2021; Ji et al., 2021; Xu et al., 2022; Zhao et al., 2022).

Figure 4 shows the TEM micrographs of the effect of HPT turns on the grain refinement of pure Mg, AZ31, and AZ80 alloys (Alsubaie et al., 2016; Gu et al., 2018; Li Y. S. et al., 2020). The results of an investigation into pure Mg processed through 1, 3, 5, and 10 HPT turns by Gu et al. (2018), show that hardness increased with the increasing equivalent strain, and then decreased to a steady-state, while the average grain size continued to decrease with the increasing equivalent strain. The minimum average grain size was 343 nm, as shown in Figure 4A. Li Y. S. et al. (2020) carried out an investigation into the microstructural and mechanical properties of Mg-Zn-Y alloys fabricated by HPT under the condition of 1/6, 1, 3, 5, and 7 turns at room temperature, with the pressure of 5.0 GPa, as shown in Figure 4B. The nanocrystalline material, with grain size of 53 nm, was prepared at 7 turns, the smallest recorded in all of the papers published about Ma-Zn-Y alloy. Meanwhile, the HPT process promoted the dissolution of MgZn and $MgZn_2$ phases. From the report of Alsubaie et al. (2016), as shown in Figure 4C, the grains of AZ80 alloys were refined from 25 μm to 200 nm after 5 and 10 turns, and the microhardness increased from 63 HV to 120 HV at the equivalent strain of 30.

3.3 Applied pressure

It has been demonstrated experimentally that the high applied pressure may have a significant impact on the grain refinement, microstructure homogeneity, and microhardness enhancement throughout the disc (Zhilyaev et al., 2001; Srinivasarao et al., 2013; Meng et al., 2014; Bazarnik et al., 2016; Gu et al., 2018). Meanwhile, high applied pressure is also crucial for generating frictional forces to hold samples and prevent the occurrence of slippage.

Srinivasarao et al. (2013) evaluated the influence of different applications of pressure (1.0, 3.0, and 6.0 GPa) on

microstructures of Mg-Li alloys. The results show that the as-received alloy, with an average grain size of 300 μm, was refined to 30–50 nm as a minimum with increasing applied pressure, and the phase transformation was also enhanced. As cited before in the research of Meng et al. (2014), and Gu et al. (2018), the experiments on pure Mg were carried out under the HPT pressure of 4.0 and 5.0 GPa, respectively. The results show equiaxed, dynamically recrystallized grains with an average size of 140 nm under the condition of 5.0 GPa, and 343 nm at 4.0 GPa after 20 turns. A similar study into the effect of applied pressure on the microstructural evolution and homogeneity of 5483 Al alloys showed that a higher pressure enhanced the generation and development of defects and a more rapid grain refinement was easily obtained. Moreover, the influence of applied pressure was more noticeable in the early stage of the HPT process, since the microstructure and microhardness tend to homogenize with increasing HPT turns (Bazarnik et al., 2016).

3.4 Rotation speed

While numerous reports establish the effects of processing temperature, turns, and applied pressure on the microstructural evolution in HPT processing of Mg alloys, only limited information is presently available on the influence of strain rate and anvil rotation speed. Most investigations have focused on samples deformed at a speed of 1 rpm (Huang et al., 2012; Meng et al., 2014; Alsubaie et al., 2016; Bazarnik et al., 2016; Lee et al., 2016; Lukyanova et al., 2016; Alsubaie et al., 2017; Gu et al., 2018; Li Y. S. et al., 2020; Ji et al., 2021). In light of the observation about Ti alloys processed by HPT from 0.5 to 2 rpm (Shahmir and Langdon, 2016), we know that the allotropic phase transformation occurred during HPT, and the volume fraction of the ω-phase decreased with the increasing rotation speed. It can be surmised hereby that the parameter of rotation speed may impact the microstructural evolution of HPTed Mg alloys more or less.

Figueiredo et al. (2017) and Figueiredo et al. (2020) carried out the HPT process on pure Mg under the condition of room temperature, using the pressure of 6.0 GPa, with rotation speeds of 2 and 1 rpm, respectively. Silva et al. (2017) conducted the HPT process on pure Mg under the same condition, except the rotation speed changed to 1 rpm. By comparing the results of these two experiments, we concluded that the lower rotation speed was beneficial for the grain boundary sliding and microstructure homogeneity, but that rotation speed had little influence on the grain size values (0.6–1.0 μm at 1 rpm, and 0.6–1.2 μm at 2 rpm).

In general, most researchers have achieved grain refinement by controlling the fundamental deformation parameters. During the HPT process, the applied strain is a major parameter affecting grain refinement and the final structure, which is mainly influenced by HPT turns. Processing temperature and applied pressure are the main factors controlling the internal energy to change grain refinement behavior and the coarsening progress. Rotation speed during the HPT process can impact microstructure homogeneity, but has little influence on grain size value. It is useful for Mg alloys processed by HPT, due to the imposition of hydrostatic pressure. Meanwhile, the whole process can be conducted at room temperature without any cracking.

4 Textural evolution of Mg alloys processed by HPT

A considerable amount of research indicates that plastic deformation significantly affects plastic anisotropy through the formation of crystallographic texture (Wang and Huang, 2003; Beausir et al., 2007; Kocich et al., 2016; Bourezg et al., 2018; Hanna et al., 2019a; Azzeddine et al., 2022). In Mg alloys, the textural anisotropy can be strong, due to the HCP structure, which will strongly influence the mechanical properties (Wang and Huang, 2003; Beausir et al., 2007). During the HPT process, the imposed magnitude of shear strain is the main factor impacting the formation of texture. Meanwhile, the texture is also affected by temperature, stress, strain rate and so on. Another influence factor is the alloying element, since these elements can modify the lattice parameters, the stacking fault energy, and the critical resolved shear stress (CRSS) for different slip systems (Azzeddine et al., 2022).

4.1 Effect of accumulative shear strain

It is generally thought that the textural evolution in Mg alloys can be expressed as a function of HPT turns, which determine the cumulative shear strain. Table 2 summarizes the textural evolution of HPTed Mg alloys as a function of HPT turns (Huang et al., 2013; Qiao et al., 2014; Lee et al., 2015; Bourezg et al., 2018; Hanna et al., 2019a; Khaleghi et al., 2021). An experiment processing pure Mg by HPT under the conditions of 6.0 GPa, 1 rpm, and at room temperature, with turns from 1/8 to 16, was carried out by Qiao et al. (2014). The initial texture was observed to be near-random, and a typical basal torsion texture was observed after 1 turn. Meanwhile, the texture features became saturated with the increasing number of HPT turns. Similar results were found in HPT processes of Mg-1.44Ce (Bourezg et al., 2018), Mg-1.43Nd (Bourezg et al., 2018), and Mg-0.41Dy (Hanna et al., 2019a). It is important to notice that the presently discussed textural features are related to position, and the center of the HPT processed discs was the position chosen. The basal torsion texture was observed in the early stages of the HPT process and this became saturated with the increasing number of HPT turns.

The weakening of basal texture occurred with the increasing cumulative shear strain. In observation of HPTed AM60 alloys (Khaleghi et al., 2021), the basal texture formed after 1 HPT turn and softened after 10 HPT turns. Moreover, the intensity and

TABLE 2 Texture evolution of HPTed Mg alloys examined in the left as a function of HPT turns.

Material	HPT parameters	Initial texture	HPTed texture	Ref
pure Mg	RT, 6.0 GPa, 1 rpm, and (1/8, 1/4, 1/2, 1, 2, 4, 8, 16) turns	Random texture	Developing the torsion texture after 1 turn, and a basal fiber texture observed after 8 turns	Qiao et al. (2014)
Mg-0.41Dy	RT, 6.0 GPa, 1 rpm, and (1/4, 1/2, 1, 5, 10, 15) turns	Random texture	Forming a basal fiber texture after 1 turn, an asymmetric split of basal planes observed due to the shear deformation with increasing HPT turns	Hanna et al. (2019a)
Mg-1.43Nd	RT, 6.0 GPa, 1 rpm, and (1/2, 1, 5, 10) turns	Random texture	Forming an asymmetric split texture of basal planes shifted towards SD.	Bourezg et al. (2018)
Mg-1.44Ce	RT, 6.0 GPa, 1 rpm, and (1/2, 1, 5, 10) turns	Random texture	Forming an asymmetric split texture of basal planes shifted towards SD.	Bourezg et al. (2018)
Mg-6Zn-0.5Zr	RT, 6.0 GPa, 1 rpm, and (1/4, 1/2, 1, 3, 5) turns	Basal extrusion texture	Forming a <c+a> fiber texture after 1/4 and 1/2 turn	Lee et al. (2015)
Mg-3Al-1Zn	(RT, 100°C, 200°C), 6.0 GPa, 1 rpm, and (1, 5) turns	Basal extrusion texture	Forming main (0001)<uvtw> fiber and a second fiber texture, and decreasing intensity observed with increasing temperature	Huang et al. (2013)

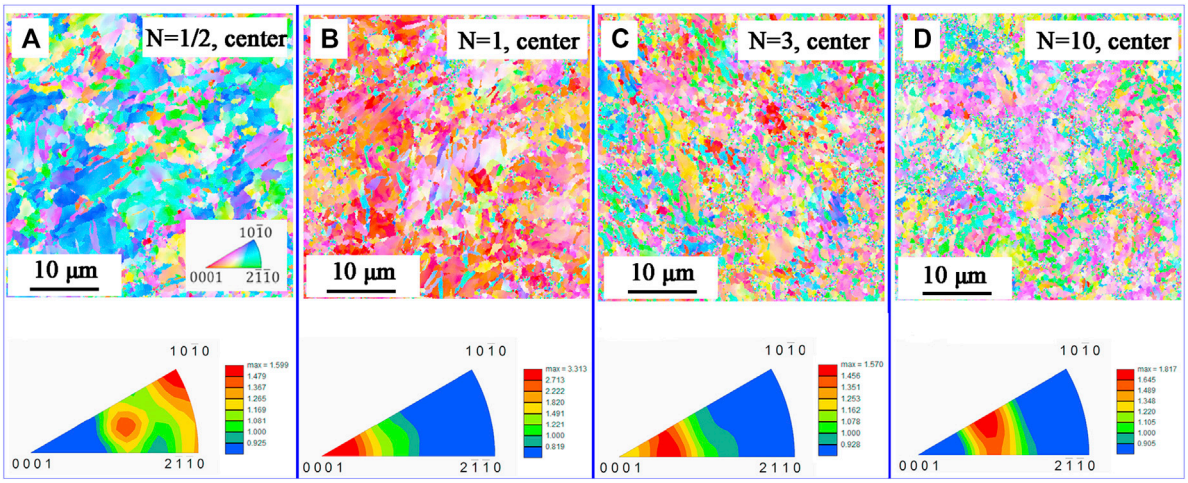

FIGURE 5
Grain orientations and inverse pole figures of AM60 alloys with **(A)** 1/2 turn, **(B)** 1 turn, **(C)** 3 turns, and **(D)** 10 turns (Khaleghi et al., 2021).

distribution of basal texture could be altered with increasing shear strain as in AM60 alloys caused by the $Mg_{17}Al_{12}$ precipitates in the HPT process. The texture evolution of HPTed AM60 alloys with different turns is shown in Figure 5 (Khaleghi et al., 2021). The formation of basal texture created a low Schmid factor for basal slip during plastic deformation at room temperature, and hence non-basal slip systems with high CRSS are needed for a significant increase in yield strength.

4.2 Effect of alloying elements

The presence of alloying elements has a significant influence on the distribution of the basal poles and the corresponding texture intensity. Bourezg et al. (2018) conducted the HPT process at room temperature with up to 10 turns of Mg-RE alloys and the texture evolution was investigated. The effect of different alloy elements on the evolution of texture is shown in Figure 6 (Bourezg et al., 2018). It can be seen that the HPTed Mg-1.44Ce and Mg-1.43Nd alloys form a weak and asymmetric basal texture, with a "crescent" form that unilaterally shifts about 15° in the shear direction (SD). Lee et al. (2015) explored the texture of ZK60A alloys, which is characterized by a shift of the basal poles towards the SD, leading to the formation of <c+a> fiber texture after HPT through 1/4 and 1/2 turns at room temperature. However, Torbati-Sarraf et al. (2017) concluded that a typical basal <a> texture is observed when 5 HPT turns are applied to ZK60A alloys. The general weakening of texture and the altering of the grain orientation with a change in alloying elements, such as rare-earth elements, is mainly related to the grain boundary

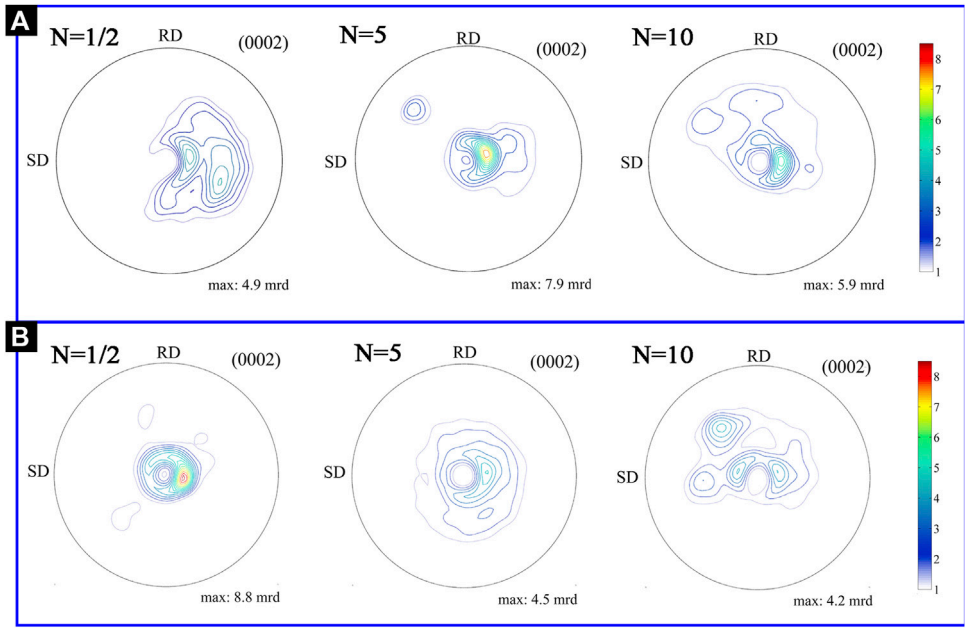

FIGURE 6
The pole figures of **(A)** Mg-1.43Nd alloys and **(B)** Mg-1.44 Ce alloys (Bourezg et al., 2018).

pinning effects caused by precipitate particles, and the activation of non-basal slip through a modification of the stacking fault energy of the Mg matrix (Jung et al., 2015; Sun et al., 2017b).

4.3 Recrystallization texture

During the HPT process, recrystallization is a typical characteristic of the deformed structure. Meanwhile, the occurrence of most recrystallized grains would impact the textural features. Until now, there are only a few research reports on the recrystallization texture evolution of Mg alloy during the HPT process (Hanna et al., 2019b; Tighiouaret et al., 2019).

Figure 7 shows the texture of HPTed Mg-Nd alloys at room temperature through 5 turns, and isochronal annealing for 1 h at 250 and 350°C, together with discussion of the resultant deformed and recrystallized texture (Tighiouaret et al., 2019). It can be seen that the deformation texture is basal, and that it shifted 60° away from the SD, and this was maintained during annealing up to 250°C. With the annealing temperature increasing to 350°C, a basal texture with symmetrical splitting towards the SD was observed. The precipitation sequence and its pinning effects were reasonable for the texture modification. Compared to Mg-1.43Nd alloys, the recrystallization texture of Mg-0.41Dy alloys appeared at a higher temperature of 400°C, which could contribute to the extensive recrystallization of grains to achieve the texture modification (Hanna et al., 2019a).

Two main fiber textures were found in Mg-0.41Dy alloys processed by HPT through 5 turns by Hanna et al. (2019b): Firstly, a basal fiber texture, and secondly, a fiber localized at φ_1 = 180°, Φ = 60°, and φ_2 = 0–90°, with the texture features retained after annealing at 400°C for 1 h. The microstructural thermal stability and microhardness values proved the stabilization of the annealed texture. Moreover, the second fiber disappeared in annealing at 200°C, and the formation of a recrystallized texture may be the main result.

Crystallographic texture affects most of the plastic anisotropy in Mg alloys, and also significantly impacts physical and engineering properties, such as formability and strength. For example, the limited formability of Mg alloys can be improved with a suitably formed texture, as reported for shear-induced texture in deformed Mg alloys (Biswas et al., 2010), and so to can MG alloys be strengthened through textural deformation.

5 Mechanical properties of ultrafine-grained Mg alloys processed by HPT

The HPT process can significantly improve the mechanical properties of nearly all kinds of metals or alloys. It has been proven that the microhardness of HPTed metals improved up to 50% for pure Mg (Gu et al., 2018), 60% for pure Cu (Edalati et al., 2008), 100% for pure Al (Harai et al., 2008b), 130% for pure Ti (Edalati et al., 2009a), and also hardened considerably for a range

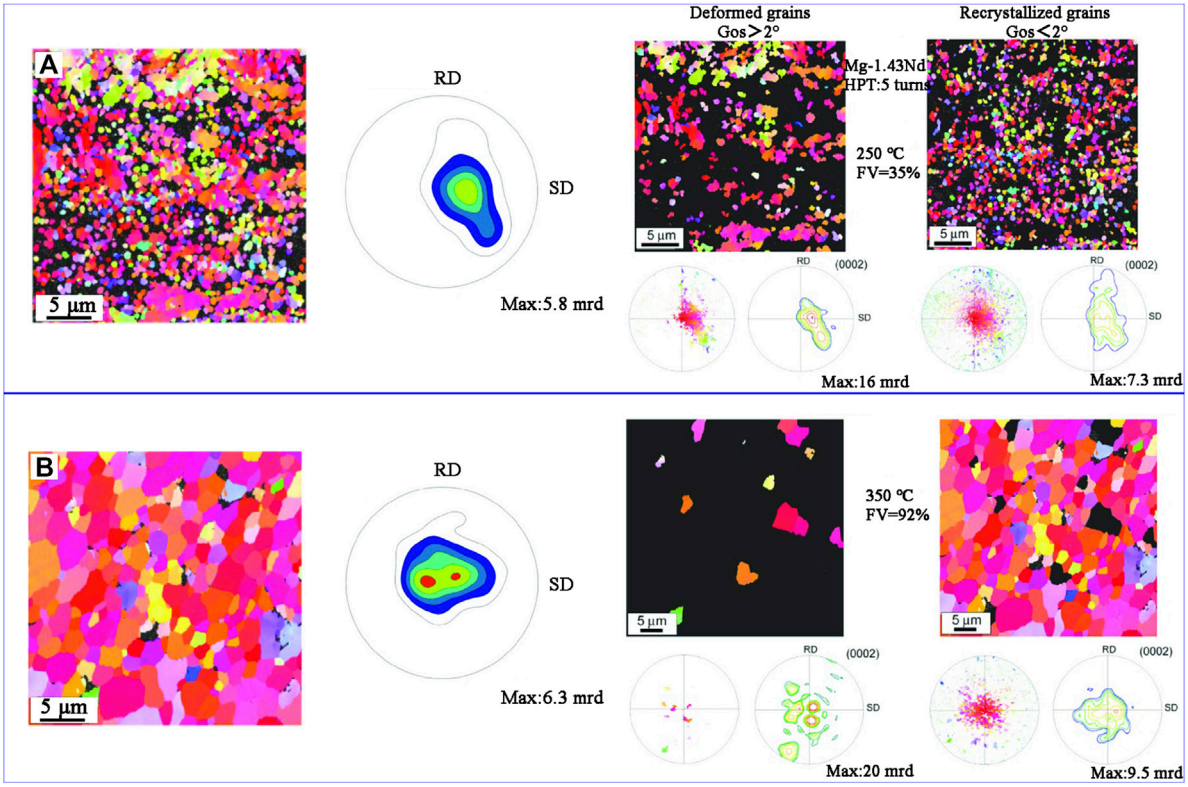

FIGURE 7
Texture of Mg-1.43Nd alloys processed by HPT after annealing at 250°C **(A)** and 350°C **(B)** (Tighiouaret et al., 2019)

of other metals (Mulyukov et al., 1991; Wei et al., 2006; Edalati et al., 2009b; Edalati et al., 2010; Popov et al., 2012b).

5.1 Improving microhardness/strength and ductility

Table 3 summarizes the mechanical properties of metals produced by SPD processes (Iwahashi et al., 1998; Munnoz-Morris et al., 2003; Peng et al., 2007; Qu et al., 2009; Edalati et al., 2010; Edalati and Horita, 2010; Kapoor et al., 2010; An et al., 2011; Kawasaki et al., 2011; Zhang et al., 2011; Popov et al., 2012b; Liu et al., 2013; Toroghinejad et al., 2013; Kawasaki et al., 2014b; Huang et al., 2014; Meng et al., 2014; Lu et al., 2015; Bazarnik et al., 2016; Zou et al., 2016; Tang et al., 2017; Čížek et al., 2017; Gu et al., 2018; Su et al., 2018; Klu et al., 2019; Xue et al., 2019; Klu et al., 2022; Öğüt et al., 2022). It can be seen that HPT processing has obvious advantages in processing metals with high strength and microhardness in comparison with other thermomechanical processing methods, such as ECAP, ARB, extrusion, and rolling. The large shear strain imposed by the HPT process generates considerable dislocations in metals or alloys, which further leads to significant grain refinement. Meanwhile, the increasing dislocation density and structure refinement can improve the microhardness of HPTed materials. Figure 8 shows the advantages of the HPT process in the YS and ductility of different metals (Qu et al., 2009; Kapoor et al., 2010; An et al., 2011; Liu et al., 2013; Toroghinejad et al., 2013; Bazarnik et al., 2016; Zou et al., 2016; Su et al., 2018; Klu et al., 2019; Klu et al., 2022). It can be seen that the HPTed Cu-16Al alloys shows an increase of 80 MPa in YS compared with the ECAPed alloys. In the investigations of Mg-9Li alloys, the ductility of HPTed alloys is 2.5 times that of the ECAPed alloys. On the whole, the advantages of HPT processing are obvious, and the significant grain refinement which comes from the high cumulative strain promotes the improvement of comprehensive mechanical properties.

A nanocrocrystalline microstructure with a grain size of 20–90 nm was observed in Mg-4.7Y-4.6Gd-0.3Zr alloys processed by HPT at room temperature or 200°C through 10 turns (Huang et al., 2012). The ultimate tensile strength was tested to be 475 MPa at an elongation of 2.5%. Moreover, the mechanical properties could be further improved by aging, and the microhardness increased during the entire aging period

TABLE 3 Mechanical properties of different alloys processed by various SPD techniques.

Material	Processing history	UTS (MPa)	YS (MPa)	Ef (%)	Hardness (MPa)	Ref
Pure Mg	HPT 4.0 GPa 20 turns	-	-	-	550	Gu et al. (2018)
Mg-3Al-1Zn	HPT 6.0 GPa 5 turns	-	-	-	1078	Kawasaki et al. (2014b)
Mg-3Al-1Zn	ECAP 4 passes	283	-	13.3	647	Öğüt et al. (2022)
Mg-3Al-1Zn	EXP.-ECAP 4 passes	292	-	13.7	666	Öğüt et al. (2022)
Mg-3.4Zn	HPT 5.0 GPa 3 turns	-	-	-	1254	Meng et al. (2014)
Mg-9Li	HPT 6.0 GPa 10 turns	220	152	55	666	Su et al. (2018)
Mg-9Li	ECAP + rolling	206	167	21	-	Klu et al. (2022)
Mg-9Li	Rolling	135	110	31	-	Zou et al. (2016)
Mg-9Li	ECAP 8 passes	166	174	22	-	Klu et al. (2019)
Mg-22Gd	HPT 2.0 GPa 15 turns	-	350	-	1431	Čížek et al. (2017)
Mg-1.8Gd-1Zn-0.1Zr	ECAP 16 passes	390	334	22.5	1166	Lu et al. (2015)
Mg-12Gd-3Y-0.4Zr	Extruded	335	248	7.8	-	Peng et al. (2007)
Mg-12Gd-3Y-0.4Zr	Extruded + rolling	396	323	10.4	-	Peng et al. (2007)
Mg-8Gd-3Y-0.4Zr	HPT 6.0 GPa 10 turns	-	-	-	1240	Tang et al. (2017)
Pure Cu	HPT 6.0 GPa 5 turns	515	440	3.4	-	An et al. (2011)
Cu-5Al	ECAP 4 passes	590	545	1.9	-	Qu et al. (2009)
Cu-16Al	HPT 6.0 GPa 5 turns	980	820	3.3	-	An et al. (2011)
Cu-16Al	ECAP 2 passes	862	740	2.2	-	Qu et al. (2009)
Pure Al	HPT 6.0 GPa 5 turns	-	-		490	Kawasaki et al. (2011)
Al-5483	HPT 6.0 GPa 3 turns	850	600	2	2000	Bazarnik et al. (2016)
Al-5083	ARB	-	560	5.7	1570	Toroghinejad et al. (2013)
Al-1Mg	HPT 3.0 GPa 16 turns	-	-	-	1860	Zhang et al. (2011)
3Al-1Mg	HPT 6.0 GPa 5 turns	440	400	-	1140	Huang et al. (2014)
Al-1Mg	ECAP 6 passes	285	250	16	-	Iwahashi et al. (1998)
Al-2.5 Mg	HPT 6.0 GPa 10 turns	670	505	2	1650	Liu et al. (2013)
Al-2.5 Mg	ECAP 4 passes	267	222	12	-	Kapoor et al. (2010)
Al-3Mg	ECAP 8 passes	510	392	-	1100	Munnoz-Morris et al. (2003)
Al-3Mg	HPT 3.0 GPa 16 turns	-	-	-	2300	Zhang et al. (2011)
Pure Ti	HPT 6.0 GPa 4 turns	-	-	-	3430	Edalati and Horita, (2010)
TA15	HPT 5.0 GPa 8 turns	-	-	-	3700	Xue et al. (2019)
Pure Hf	HPT 4.0 GPa 10 turns	1150	-	8	3528	Edalati et al. (2010)
Pure Nb	HPT 6.0 GPa 5 turns	-	-	-	3100	Popov et al. (2012b)
Pure Nb	ECAP 16 passes	-	-	-	2180	Popov et al. (2012b)
Pure Nb	ECAP + HPT	-	-	-	3150	Popov et al. (2012b)

ARB, accumulative rolling bonding pressing; EXP.-ECAP, expansion equal channel angular extrusion pressing; UTS, ultimate tensile strength; YS, yield strength; Ef, elongation to failure.

at 175°C, reaching a "quasi-steady" state corresponding to 1600 MPa. The nanostructured Mg-8.2Gd-3.2Y-1.0Zn-0.4Zr alloy, with an average grain size of 35 nm, was produced by Sun et al. (2018), and the ultra-high hardness of 156 HV was achieved by a combination of HPT processing and aging treatment, which was higher than any Mg alloys hitherto reported in the literature. The hardening of grain refinement, high dislocation density, and solute segregation contributed simultaneously to the high microhardness. Hardness evolution into ultrafine-grained Mg-3.4Zn alloys processed by HPT is predominantly influenced by crystalline defects, grain size, and precipitates (Meng et al., 2015). The greatest hardness was obtained via ultrafine-grained structural and grain boundary precipitates possessing high density dislocations and defects. Recovery of defects and grain growth led to decreasing hardness at the aging temperature of 150°C.

5.2 Deformation mechanisms

5.2.1 Grain boundary sliding

The strong ability of the HPT process is in preparing ultrafine-grained materials, and a high volume fraction of grain boundaries with decreasing grain size can be obtained

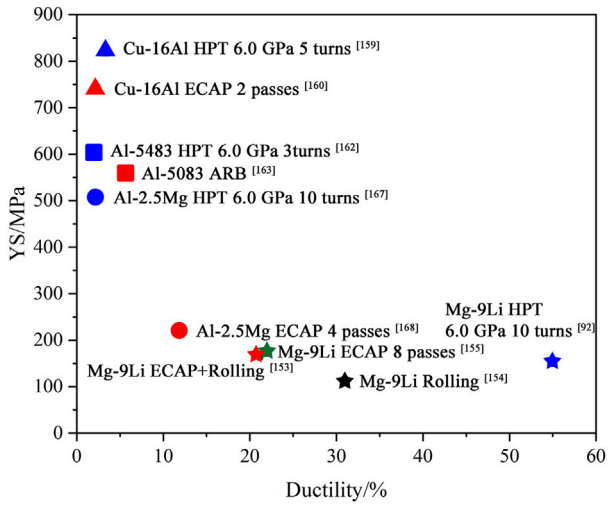

FIGURE 8
The comparison of metal processed by various SPD techniques in YS and ductility (Qu et al., 2009; Kapoor et al., 2010; An et al., 2011; Liu et al., 2013; Toroghinejad et al., 2013; Bazarnik et al., 2016; Zou et al., 2016; Su et al., 2018; Klu et al., 2019; Klu et al., 2022).

during the process. Grain boundary sliding can be activated, since the grain size is below a critical value. This is beneficial for high comprehensive mechanical properties, and may even result in superplasticity. Matsunoshita et al. (2015) report a HPTed Mg-8Li alloy with an average grain size of 500 nm showing an elongation of 310% at room temperature, and 1330% at 200 °C. The superplasticity of Mg-8Li alloys is mainly based on grain boundary sliding.

5.2.2 Slip and twinning

The von Mises criterion mentions that to avoid cracking, plastic deformation for polycrystalline materials need to satisfy the condition of five independent slip systems. However, basal <a> is the common slip system for Mg alloys, and the other independent slip systems are prismatic and pyramidal <a> slips. A large CRSS is needed to start the < c+a> slip system. In the deformation process, twinning can help to solve the problem of hard-to-deform Mg alloys. The common observed twinning feature in Mg alloys is (10–12), which is called tension twinning, due to it causing an extension along the *c*-axis when activated, as Mg experiences tension stress along the *c*-axis. In the compression samples (10–11), twinning is often observed.

For Mg alloys, during deformation the activation of slip systems and twinning basically depends on the CRSS, activation stress, and the Schmid factor. In the report of Qiao et al. (2014), cited previously, the as-cast pure Mg, basal <a> and non-basal < c+a> were slip activated rather than through twinning, because the as-cast pure Mg had no preferential texture features, and the basal plane was distributed randomly. Hence the Schmid factor did not favor the tension and twinning was suppressed. The double textures were observed afterward as-cast pure Mg processed by 1/8 turn, and the non-basal < c+a> slip was activated along with the basal <a> slip.

For the extruded Mg, because of the existence of basal planes parallel to the extrusion direction and perpendicular to the shear direction, a large number of twins were observed after 1 turn. In this instance, the Schmid factor of the basal planes was zero, and (10–12) twinning was 0.5. Tension twinning was thus activated when the basal slip was hindered (Xu and Han, 2013). With increasing HPT turns, dislocation slip became the dominant mechanism because of the rotation of the basal planes and coordination of the twinning. Similarly, extension twinning (10–12) <10–11> was most extensive in the samples of Mg-Dy-Al-Zn-Zr alloys processed by HPT (Nie et al., 2010).

5.3 Strengthening mechanisms

5.3.1 Grain refinement strengthening

Grain refinement is the most effective means of improving the mechanical properties of Mg alloys in the HPT process. It can increase both yield strength and plasticity, and the relationship between grain size and yield strength can be expressed by the Hall–Petch criterion (Chen et al., 2016):

$$\sigma_y = \sigma_0 + kd^{-1/2} \quad (2)$$

where σ_y is the yield strength, σ_0 is the yield strength of a single crystal of Mg, k is the coefficient, and d is the average grain diameter. It can be obtained from the equation that the σ_y would increase with the decreasing d.

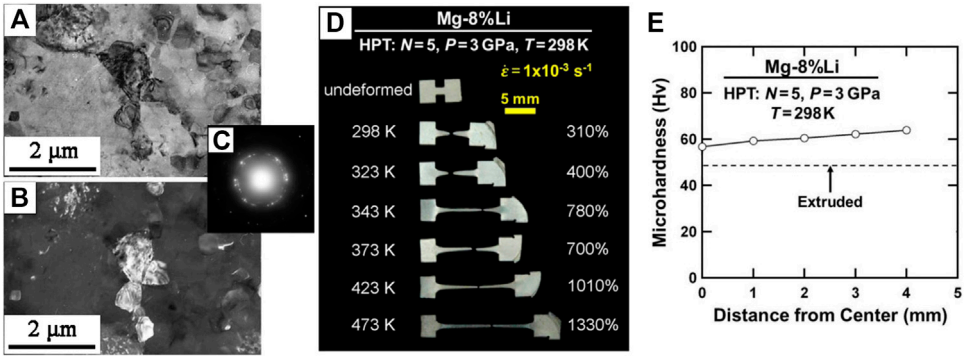

FIGURE 9
TEM observation of Mg-8Li alloys after 5 HPT turns **(A–C)**, tensile elongation of HPTed samples after different temperatures with the strain rate of 1×10^{-3} s^{-1} **(D)**, and microhardness of different positions **(E)** (Matsunoshita et al., 2015).

According to metallic theory, the number of grain boundaries will increase with the increasing volume fraction of grains per unit. The grain boundaries can effectively hinder the dislocation movement, and this can improve the physical mechanical properties of Mg alloys (Peng et al., 2022). Figure 9 shows some investigative results from Matsunoshita et al. (2015) of Mg-8Li alloys processed by HPT through 5 turns at room temperature. It can be seen that 500 nm ultrafine grains were observed, and the superplastic elongation of 1330% was investigated at 200°C with the strain rate of 1×10^{-3} s^{-1}. The microhardness of the HPTed sample was 57–63 HV, which was much higher than for the as-extruded bar. The significant improvement in mechanical properties was mainly produced by the grain boundary refining and sliding. A similar strengthening effect of ultrafine-grained LZ91 Mg-Li alloys is reported by Su et al. (2018). Figure 10 shows the TEM observation of ultrafine grains and the microhardness evolution of LZ91 alloys (Su et al., 2018). It can be seen that the 230 nm LZ91 Mg-Li alloy was papered after HPT through 10 turns at room temperature. The grain size value decreased with the increasing HPT turns, while the microhardness increased. The relationship between the average diameter and microhardness satisfied the Hall–Petch strengthening criterion. Moreover, the superplastic tensile elongation of 400% at 200°C was observed with the strain rate of 1×10^{-2} s^{-1}.

5.3.2 Secondary phase strengthening (precipitation strengthening)

Because of their dimensions and properties, secondary phases can strengthen the Mg matrix by acting as obstacles hindering the dislocation movement. The Orowan mechanism can be used to quantitatively analyze the contribution of secondary phase particles to strength.

$$\Delta\sigma_0 = \sqrt{3}\,(Gb/L) \tag{3}$$

where G is the shear modulus, b is the Burgers vector, and L is the average distance among the secondary phase particles. In Mg alloys, the size and morphology of secondary phases are the main factors affecting the strengthening results. The fine and dispersed particles create an important increasing mechanical property, while the continuous and inhomogeneous distribution of secondary phases result in decreasing strength and ductility.

Figure 11 shows the nanostructured Mg-4.97Sm-0.84Ca alloy processed by HPT through 4 turns at room temperature (Liu et al., 2020). The greatest hardness reached 145 HV after aging treatment at 125°C for 8 h. The precipitation strengthening of nanoscale precipitates contributed to the increasing microhardness, and the competition of recrystallization softening also affected the final properties. Similar research was conducted by Meng et al. (2015). The precipitates of Mg-3.4Zn alloys after the HPT process and aging treatment were distributed on the grain boundaries, and a precipitate-free-zone (PFZ) was formed along the boundaries, which strengthened the matrix and hindered the grain boundary from sliding, resulting in an increasing microhardness.

Besides the significant impact of aging precipitates, the dynamic precipitation during hot deformation also played an important role in the mechanical properties of Mg alloys. In the research of Xiao et al. (2015), the equilibrium β phase particles distributed along the grain boundaries formed necklace structures at 350°C with the strain rate of 0.001–1 s^{-1}. Meanwhile, the TEM observation proved that the existence of dynamic precipitates promotes the formation of subgrains, and impedes the migration of DRX grain boundaries.

5.3.3 Solid solution strengthening

For engineering Mg alloys, the addition of rare-earth (RE) elements to obtain the Mg-RE alloy, which has higher mechanical properties than the traditional commercial Mg alloys, is a

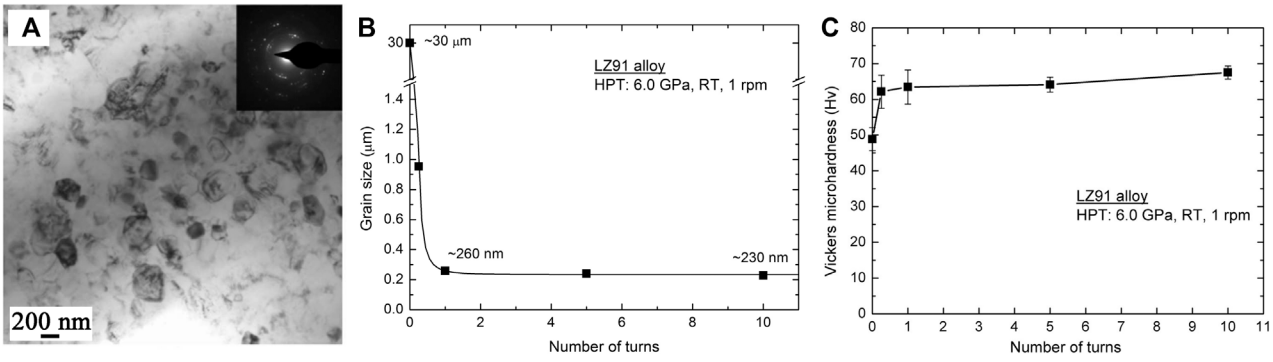

FIGURE 10
TEM observation of ultrafine-grained Mg-Li alloys after 10 HPT turns **(A)**, the relationship between grain size **(B)**, or microhardness **(C)**, and the number of turns (Su et al., 2018).

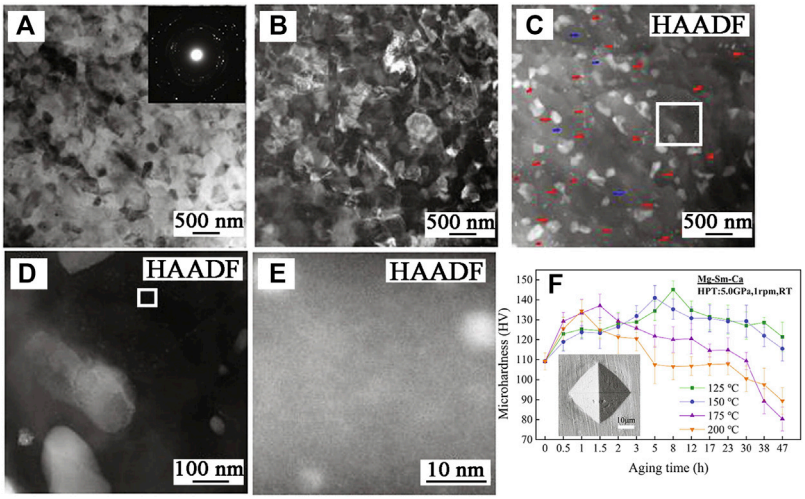

FIGURE 11
Microstructure of Mg-Sm-Ca alloys processed by HPT and aging treatment at 125°C for 8 h: **(A)** TEM bright-field micrograph; **(B)** TEM dark-field micrograph; **(C)** HAADF-STEM micrograph; **(D)** high magnification HAADF-STEM micrograph of white spot in **(C)**; **(E)** high magnification HAADF-STEM micrograph of white spot in **(D)**; **(F)** microhardness of different aging conditions (Liu et al., 2020).

promising route for promoting the application of Mg alloy products to the aerospace and defense industries. RE elements, such as Gd and Y, have a relatively high solid solubility in the Mg matrix (Yan et al., 2021), and RE atoms can replace Mg atoms and enter the Mg lattice structure, causing the distortion. Thus, solid solution strengthening may be a method for further improving the strength of some Mg alloys. The influence of an element solid solution is expressed as the following equation (Zhang et al., 2019):

$$\sigma = \alpha G b \rho^{1/2} \quad (4)$$

where α is the material constant, and ρ is the dislocation density.

Li et al. (2019) investigated the microstructural evolution and mechanical properties of Mg-13Gd-4Y-2Zn-0.6Zr alloys processed by multi-pass hot rolling with different accumulated rolling reductions. The contribution of tensile yield strength was divided into five kinds, and the solid solution strengthening was calculated to be 40 MPa. A familiar investigation was conducted by Yao et al. (2019), in which the Gd, Y and Zn solute atoms dissolution were estimated according to the results of EDS, and the contribution from Gd, Y and Zn of the extruded Mg-1.4Gd-1.2Y-0.4Zn alloy were calculated to be 148 MPa.

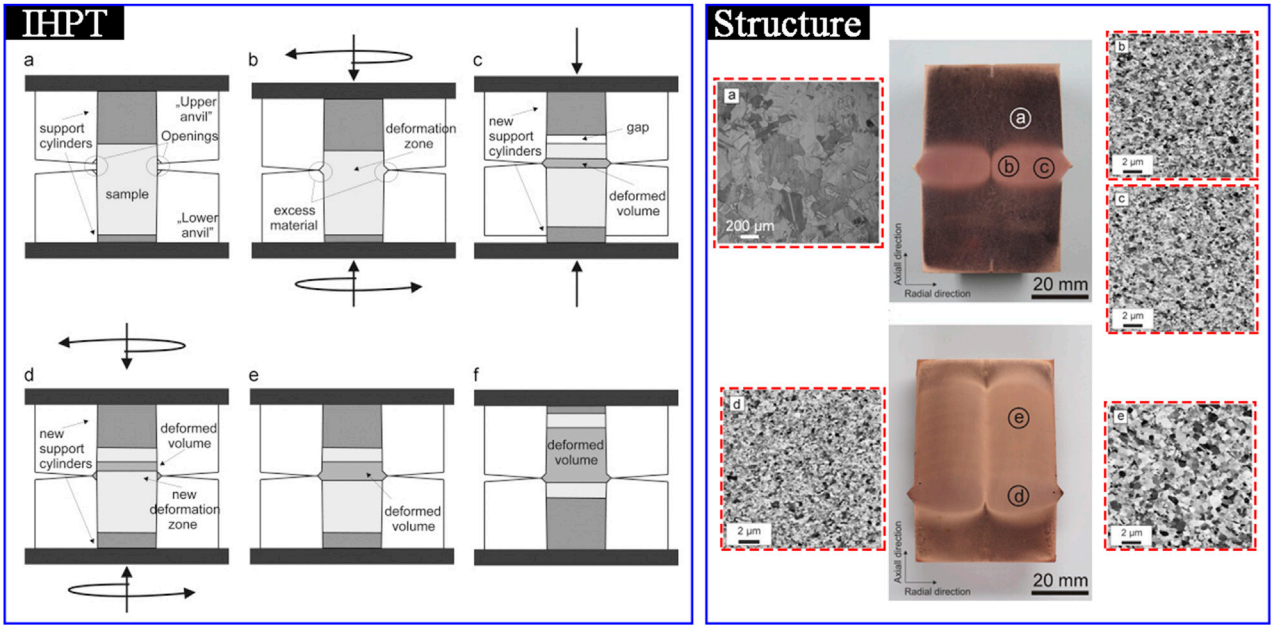

FIGURE 12
Schematic of IHPT process and its processed copper with microstructures in different positions (Hohenwarter, 2015).

5.3.4 Texture strengthening

Crystallographic texture is a typical behavior of the preferred orientation of most grains in a polycrystal aggregate. For Mg alloys with HCP structure, the preferred grain orientations usually occur during plastic deformation, which is called "deformation texture." The textural features can be dictated by the initial grain orientation and the deformation method imposed (Suwas and Soumita, 2019). In the HPT process, a typical shear texture is formed because of the shear-based processes (Kloden et al., 2007; Bonarski et al., 2008a; Bonarski et al., 2008b; Khereddine et al., 2013; Jahedi et al., 2014; Basha et al., 2016; Li et al., 2016; Wei et al., 2017; Skrotzki et al., 2020), while a basal fiber texture is observed in the rolling process, due to the imposed plane strain (Liu et al., 2018).

Texture strengthening may play a dominant role in Mg alloys and has been extensively reported. For example, texture formation in AZ31 alloys contributes greatly to yield strength (Kim and Jeong, 2005). For pure Mg (Torbati-Sarraf et al., 2017), although grain refinement and dislocation strengthening are the major strengthening options, the hardness anisotropy is related to the texture.

The changing of textural features is usually influenced by deformation direction, and the specific texture strengthening of Mg alloys is generally obtained by deformation along the forming direction, which limits the basal slip systems and is beneficial in activation of the non-basal slip systems, leading to increasing yield strength. For the HPT or ECAP processes, a shear-induced texture is the typical characteristic, and the formation of shear-induced texture can effectively promote the ductility of Mg alloys compared to the basal texture formed through extruding and rolling (Lei et al., 2017; Akbaripanah et al., 2021; Liu and Xu, 2022). Meanwhile, the mechanical anisotropy is eliminated also. Torbati-Sarraf et al. (2015) investigated the strengthening mechanism of ZK60 alloys processed by HPT through 5 turns at room temperature. They found that the high value of average microhardness (124 HV) was due to the contribution of high density dislocations, nano grain size, and strong texture strengthening.

The influence of texture on the yield strength in HCP alloys is obtained from the changing Hall–Petch constants. The contribution of texture strengthening can be calculated by the following equation (Cheng et al., 2014):

$$\boldsymbol{\varepsilon}_0 = \boldsymbol{m}\boldsymbol{\tau}_0 \tag{5}$$

where m is related to the basal texture and can be calculated by the texture intensity. If the alloy has a random texture, the m is 6.5. However, the specific texture formed through extruding, upsetting, and rolling will have a value larger than 6.5. The τ_0 is the single crystal resolved stress. Cheng et al. (2014) estimated the contribution of texture strengthening of Mg-8Sn and Mg-8Sn-1Al-1Zn alloys using AZ31 alloys as the benchmark, and the contribution values of 2.77 and 3.61 MPa were calculated, respectively.

6 Novel HPT processes

It has been 40 years since the ultrafine-grained materials were first produced by Valiev et al. in the 1980s. The reports on HPT

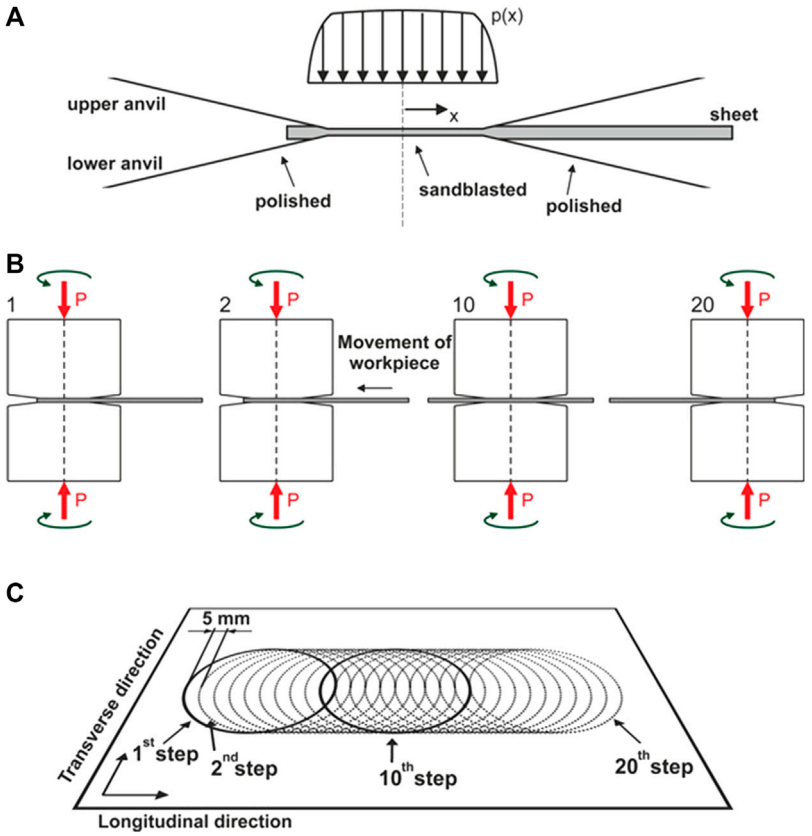

FIGURE 13
Principle of P-HPT process. **(A)** Schematic of the anvil and pressure distribution on the sheet; **(B)** representation of several P-HPT steps; **(C)** deformation zone on the sheet with increasing deformation steps (Hohenwarter and Pippan, 2018).

have demonstrated the advantages of this process for grain refinement, dislocation accumulation, texture modification, and strength improvement. However, the single shape and small size of the sample limits the industrial application of the HPT process, which remains experimental. Recently, many researchers have developed novel or modified processes based on the principles of HPT to improve processing versatility and have made various contributions.

In response to the limitation of sample size, especially the thickness of the processed samples of conventional HPT, Hohenwarter (2015) developed a novel plastic deformation process called incremental high-pressure torsion (IHPT), which was capable of delivering samples with an extraordinarily high aspect-ratio of thickness to diameter, and the principle of this technique is shown in Figure 12 (Hohenwarter, 2015). The author thought it possible to produce large samples in three dimensions with an ultrafine or nanocrystalline microstructure. This might have a bright application future in the medical or electronic fields, in which SPD processed materials have been favored until now. In his experiment, pure copper, 70 mm in height and 50 mm in diameter, was subjected to the IHPT process with a hydraulic pressure of 4 MN and rotational speed of 0.07 per minute. Finally, a processed sample with a diameter of 50 mm and a thickness of 40 mm was obtained, and an ultrafine-grained structure was observed in all dimensions.

Sheets are widely used in structural and functional areas, and microstructural modification has so far not been attempted using HPT due to the deformation characteristic. By introducing the large shear strain into materials with planar geometries, planar high-pressure torsion (P-HPT) was proposed as a modification of the conventional HPT process to fabricate the sheets and strips (Hohenwarter and Pippan, 2018). The principal diagram of the P-HPT process is given in Figure 13 (Hohenwarter and Pippan, 2018). This research introduced an adapted version of HPT, also capable of processing large-scale sheets by using a modification of conventional HPT, and proved the advantages of P-HPT on the microstructural and mechanical properties of pure copper by comparison with conventional HPT.

Increasing the strain rate is known to be an effective way of achieving grain refinement and improving mechanical

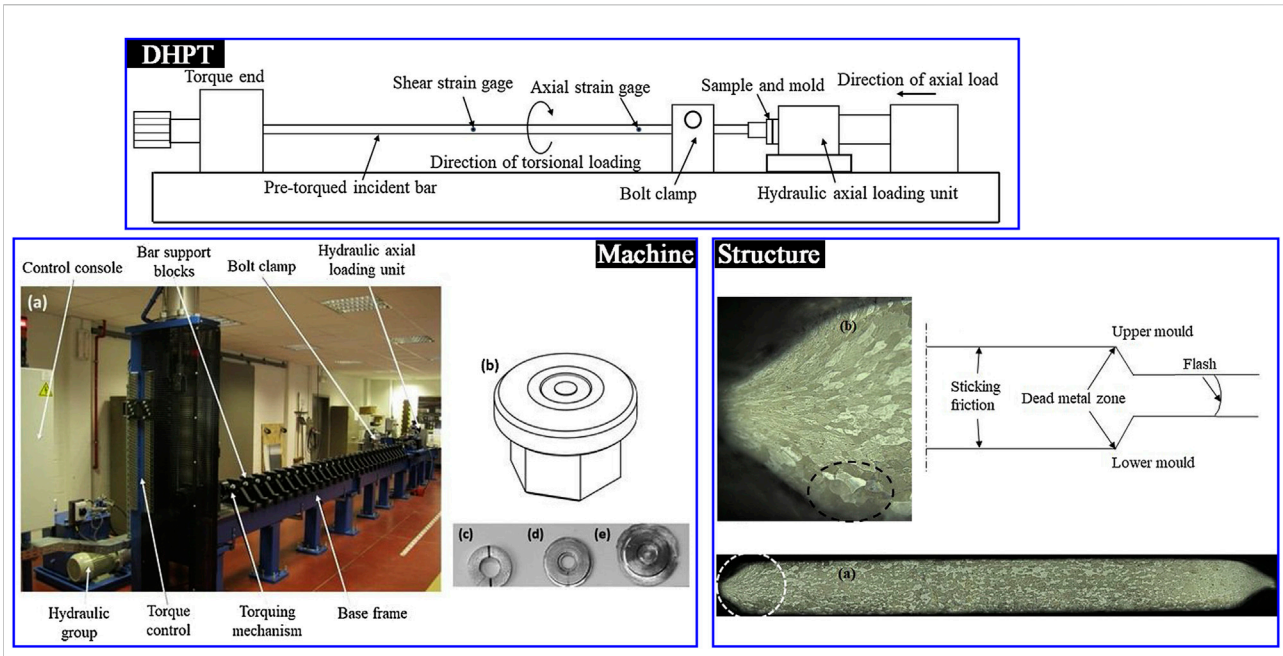

FIGURE 14
Illustration of DHPT, the used machine, and resultant microstructures of pure Al (Verleysen and Lanjewar, 2020).

properties. Verleysen and Lanjewar (2020) proposed a dynamic SPD technique which combined features of both the split Hopkinson torsion bar (SHTB) and static HPT devices, called dynamic high-pressure torsion (DHPT). The schematic diagram of this process, machine, and processed microstructure is found in Figure 14 (Verleysen and Lanjewar, 2020). This novel process first imposed a compressive pressure on a disk-like or ring-like sample placed between two molds, followed by a rotational deformation. Compared to the conventional HPT process with a rotational speed of 1 rpm in common, a relatively high torsional speed of 30,000 rpm and strain rates of 10000/s can be applied to the testing materials during DHPT. Thus, the power density of DHPTed materials can be four orders of magnitude higher than static HPTed alloys, resulting in out-of-equilibrium microstructures and new combinations of properties. In the verification experiment of pure Al, a fine grain structure of pure Al processed by DHPT was obtained, and the enhanced dislocation structure and low angle grain boundaries produced a significant improvement in microhardness.

7 Summary and conclusion

A considerable number of research studies have indicated that HPT is one of the most effective techniques for preparing ultrafine-grained Mg alloys. In this report, the HPTed Mg alloys and the resultant microstructural evolution, texture, and mechanical properties are reviewed. The main influences on the formation of ultrafine grains, crystallographic texture evolution, deformation mechanisms, and strengthening mechanisms are discussed, and the following findings can be drawn:

1) HPT processing parameters play an important role in microstructural evolution, especially grain refinement. The nanocrystalline Mg alloys can be produced by HPT, according to nearly all reports. Normally the decreasing grain sizes and refinement of precipitates are mainly impacted by processing temperature, turns, and applied pressure, while reports on the effect of rotation speed are limited. Most recent investigations chose 1 rpm to complete their HPT process, which may be astricted by the machine. Other conditions being equal, low deformation temperature and high compressive pressure with increasing HPT turns facilitate the obtaining of ultrafine grains and secondary phases. In the future, the exact influence of rotation speed on microstructural modification of Mg alloys may attract more and more attention from researchers.
2) For Mg alloys, whatever the grain orientation of the initial structure, a basal torsion texture is often developed after the HPT process according to the published data available to date. With the increasing cumulative shear strain (HPT turns), the inclination and spread of the basal poles is observed. The deviation of basal texture from its ideal position also depends on the composition of the alloy elements. Moreover,

crystallographic texture has a significant influence on the mechanical properties of Mg alloys. The limited formability can be improved by the shear-induced texture, and the deformation texture can effectively increase the strength on loading direction.

3) The Mg alloy processed by HPT shows a significant enhancement in mechanical properties due to grain refinement, strong cumulative shear strain, high density dislocation, dispersed precipitates, and so on. In view of the contribution of various strengthening mechanisms to the improvement of strength in deformed Mg alloys, grain refinement strengthening and precipitate strengthening are generally considered the main influencing factors.
4) To solve the shortcomings of the conventional HPT process and extend its industrial application, novel and modified HPT techniques such as IHPT, P-HPT, and DHPT are reported to have similar deformation advantages on microstructure and property enhancement as those formed by conventional HPT, and are also more versatile.

Overall, this review confirms that HPT processing induces considerable changes in the microstructure and texture of different Mg alloys. Crucial information about the strain-induced changes in mechanical properties, and the corresponding strengthening and toughening mechanisms, are directly linked and arise from these results. Therefore, a serious challenge is now being tackled through research investigations on the topics of dislocations, subgrain boundaries, and secondary phase particles and sizes. Also, the relationships among processing parameters, microstructure evolution, and mechanical properties have not yet been satisfactorily quantified. It is also of primary importance to develop model calculations of microstructural and textural evolution, which could be combined with the experimental results to analyze the deformation mechanisms, as well as the strengthening and toughening mechanisms. To date, most investigations focus on experimental analyses, with limited reports on the establishment of HPT model calculations.

As a final comment, the main purpose of such activity would be to achieve the application of HPT processing. Thus, an improved new technique is urgently to solve the problems of small-scale production, heterogeneous deformation, and high equipment requirements.

Author contributions

ZY and YX conceived and designed the structure of this review. ZY, JZ, ZZ, and QW wrote the manuscript.

Funding

This work was funded by the Natural Science Foundation of China under grant no. 52075501, and the Fundamental Research Program of Shanxi Province under grant no. 20210302124206.

Acknowledgments

The authors would like to acknowledge the Natural Science Foundation of China under grant no. 52075501, and the Fundamental Research Program of Shanxi Province under grant no. 20210302124206.

Conflict of interest

The authors declare that the research was conducted in the absence of any commercial or financial relationships that could be construed as a potential conflict of interest.

Publisher's note

References

Abd El Aal, M. I. (2021). The influence of ECAP and HPT processing on the microstructure evolution, mechanical properties and tribology characteristics of an Al6061 alloy. *J. Mat. Res. Technol.* 9 (6), 12525–12546. doi:10.1016/j.jmrt.2020.08.099

Akbaripanah, F., Sabbaghian, M., Fakhar, N., Minárik, P., Veselý, J., Hung, P. T., et al. (2021). Influence of high pressure torsion on microstructure evolution and mechanical properties of AZ80/SiC magnesium matrix composites. *Mater. Sci. Eng. A* 826, 141916. doi:10.1016/j.msea.2021.141916

Al-Zubaydi, A. S. J., Zhilyaev, A. P., Wang, S. C., Kucita, P., and Reed, P. A. S. (2016). Evolution of microstructure in AZ91 alloy processed by high-pressure torsion. *J. Mat. Sci.* 51, 3380–3389. doi:10.1007/s10853-015-9652-2

Alhamidi, A., and Horita, Z. (2015). Grain refinement and high strain rate superplasticity in alumunium 2024 alloy processed by high-pressure torsion. *Mater. Sci. Eng. A* 622, 139–145. doi:10.1016/j.msea.2014.11.009

Alsubaie, S. A., Bazarnik, P., Lewandowska, M., Huang, Y., and Langdon, T. G. (2016). Evolution of microstructure and hardness in an AZ80 magnesium alloy processed by high-pressure torsion. *J. Mat. Res. Technol.* 5 (2), 152–158. doi:10.1016/j.jmrt.2015.11.006

Alsubaie, S. A., Huang, Y., and Langdon, T. G. (2017). Hardness evolution of AZ80 magnesium alloy processed by HPT at different temperatures. *J. Mat. Res. Technol.* 6 (4), 378–384. doi:10.1016/j.jmrt.2017.05.004

An, X. H., Lin, Q. Y., Wu, S. D., Zhang, Z. F., Figueiredo, R. B., Gao, N., et al. (2011). The influence of stacking fault energy on the mechanical properties of nanostructured Cu and Cu-Al alloys processed by high-pressure torsion. *Scr. Mat.* 64 (10), 954–957. doi:10.1016/j.scriptamat.2011.01.041

Azzeddine, H., Bradai, D., Baudin, T., and Langdon, T. G. (2022). Texture evolution in high-pressure torsion processing. *Prog. Mat. Sci.* 125, 100886. doi:10.1016/j.pmatsci.2021.100886

Basha, D. A., Sahara, R., Somekawa, H., Rosalie, J. M., Singh, A., and Tsuchiya, K. (2016). Interfacial segregation induced by severe plastic deformation in a Mg-Zn-Y alloy. *Scr. Mat.* 124, 169–173. doi:10.1016/j.scriptamat.2016.07.021

Bazarnik, P., Romelczyk, B., Huang, Y., Lewandowska, M., and Langdon, T. G. (2016). Effect of applied pressure on microstructure development and homogeneity in an aluminium alloy processed by high-pressure torsion. *J. Alloys Compd.* 688, 736–745. doi:10.1016/j.jallcom.2016.07.149

Bazzarnik, P., Romelczyk, B., Huang, Y., Lewandowska, M., and Langdon, T. G. (2016). Effect of applied pressure on microstructure development and homogeneity in an aluminium alloy processed by high-pressure torsion. *J. Alloys Compd.* 688, 736–745. doi:10.1016/j.jallcom.2016.07.149

Beausir, B., Tóth, L. S., and Neale, K. W. (2007). Ideal orientations and persistence characteristics of hexagonal close packed crystals in simple shear. *Acta Mat.* 55 (8), 2695–2705. doi:10.1016/j.actamat.2006.12.021

Bednarczyk, W., Kawałko, J., Watroba, M., Gao, N., Starink, M. J., Bała, P., et al. (2020). Microstructure and mechanical properties of a Zn-0.5Cu alloy processed by high-pressure torsion. *Mater. Sci. Eng. A* 776, 139047. doi:10.1016/j.msea.2020.139047

Belyakov, A., Sakai, T., and Miura, H. (2000). Fine-grained structure formation in austenitic stainless steel under multiple deformation at $0.5T_m$. *Mat. Trans. JIM* 41, 476–484. doi:10.2320/matertrans1989.41.476

Biswas, S., Dhinwal, S. S., and Suwas, S. (2010). Room-temperature equal channel angular extrusion of pure magnesium. *Acta Mat.* 58 (9), 3247–3261. doi:10.1016/j.actamat.2010.01.051

Bonarski, B. J., Mikulowski, B., Schafler, E., Holzleithner, C., and Zehetbauer, M. J. (2008). Crystallographic textures of single and polycrystalline pure Mg and Cu subjected to HPT deformation. *Arch. Metall. Mater* 53 (1), 117–123. http://www.imim.pl/files/archiwum/Vol1_2008/artykuly/19_.pdf.

Bonarski, B. J., Schafler, E., Mingler, B., Skrotzki, W., Mikulowski, B., and Zehetbauer, M. J. (2008). Texture evolution of Mg during high-pressure torsion. *J. Mat. Sci.* 43 (23-24), 7513–7518. doi:10.1007/s10853-008-2794-8

Borchers, C., Garve, C., Tiegel, M., Deutges, M., Herz, A., Edalati, K., et al. (2015). Nanocrystalline steel obtained by mechanical alloying of iron and graphite subsequently compacted by high-pressure torsion. *Acta Mat.* 97, 207–215. doi:10.1016/j.actamat.2015.06.049

Bourezg, Y. I., Azzeddine, H., Baudin, T., Helbert, A. L., Huang, Y., Bradai, D., et al. (2018). Texture and microhardness of Mg-Rare Earth (Nd and Ce) alloys processed by high-pressure torsion. *Mater. Sci. Eng. A* 724, 477–485. doi:10.1016/j.msea.2018.03.114

Bridgman, P. W. (1941). Explorations toward the limit of utilizable pressures. *J. Appl. Phys.* 12, 461–469. doi:10.1063/1.1712926

Bridgman, P. W. (1940). New high pressures reached with multiple apparatus. *Phys. Rev.* 57, 342–343. doi:10.1103/physrev.57.342

Bridgman, P. W. (1911a). The action of mercury on steel at high pressures. *Proc. Am. Acad. Arts Sci.* 46, 325–341. doi:10.2307/20022653

Bridgman, P. W. (1909a). The measurement of high hydrostatic pressure. I. A simple primary gauge. *Proc. Am. Acad. Arts Sci.* 44, 201–217. doi:10.2307/20022420

Bridgman, P. W. (1909b). The measurement of high hydrostatic pressure. II. A secondary mercury resistance gauge. *Proc. Am. Acad. Arts Sci.* 44, 221–251. doi:10.2307/20022424

Bridgman, P. W. (1911b). The measurement of hydrostatic pressures up to 20000 kilograms per square centimeter. *Proc. Am. Acad. Arts Sci.* 47, 321–343. doi:10.2307/20022746

Cepeda-Jiménez, C. M., Orozco-Caballero, A., García-Infanta, J. M., Zhilyaev, A. P., Ruano, O. A., and Carreño, F. (2014). Assessment of homogeneity of the shear-strain pattern in Al-7 wt%Si casting alloy processed by high-pressure torsion. *Mater. Sci. Eng. A* 597, 102–110. doi:10.1016/j.msea.2013.12.072

Champion, Y., Couzinie, J. P., Nenez, S. T., Brechet, Y., Islamgaliev, R. K., and Valiev, R. Z. (2010). High strength and electrical conductivity of UFG copper alloys. *Mater Sci. Forum* 667-669, 755–759. doi:10.4028/www.scientific.net/msf.667-669.755

Chen, Y., Gao, N., Sha, G., Ringer, S. P., and Starink, M. (2016). Microstructural evolution, strengthening and thermal stability of an ultrafine-grained Al-Cu-Mg alloy. *Acta Mat.* 109, 202–212. doi:10.1016/j.actamat.2016.02.050

Chen, Y. H., Wang, L. P., Feng, Y. C., Guo, E. J., Zhao, S. C., Wang, L., et al. (2019). Effect of Ca and Sm combined addition on the microstructure and elevated-temperature mechanical properties of Mg-6Al alloys. *J. Mat. Eng. Perform.* 28 (5), 2892–2902. doi:10.1007/s11665-019-04044-9

Cheng, W. L., Tian, Q. W., Yu, H., Zhang, H., and You, B. S. (2014). Strengthening mechanisms of indirect-extruded Mg-Sn based alloys at room temperature. *J. Magnesium Alloys* 2 (4), 299–304. doi:10.1016/j.jma.2014.11.003

Ciuca, O., Tsuchiya, K., Yokohama, Y., Todaka, Y., and Umemoto, M. (2010). Heterogeneous process of disordering and structural refinement in Ni_3Al during severe plastic deformation by high-pressure torsion. *Mat. Trans.* 51, 14–22. doi:10.2320/matertrans.mb200915

Čížek, J., Hruška, P., Vlasák, T., Vlček, M., Janeček, M., Minárik, P., et al. (2017). Microstructure development of ultra fine grained Mg-22 wt%Gd alloy prepared by high pressure torsion. *Mater. Sci. Eng. A* 704, 181–191. doi:10.1016/j.msea.2017.07.100

Cizek, J., Janecek, M., Srba, O., Kuzel, R., Barnovska, Z., Prochazka, I., et al. (2011). Evolution of defects in copper deformed by high-pressure torsion. *Acta Mat.* 59, 2322–2329. doi:10.1016/j.actamat.2010.12.028

Danilenko, V. N., Kiekkuzhina, L. U., Parkhimovich, N. Y., Khafizova, E. D., and Gunderov, D. V. (2021). Cu-Al metal matrix composite fabricated by accumulative HPT. *Mat. Lett.* 300, 130240. doi:10.1016/j.matlet.2021.130240

de Oliveira, P. C., Montoro, L. A., Perez-Prado, M. T., Hohenwarter, A., Figueiredo, R. B., and Isaac, A. (2021). Development of segregations in a Mg-Mn-Nd alloy during HPT processing. *Mater. Sci. Eng. A* 802, 140423. doi:10.1016/j.msea.2020.140423

Dheda, S. S., and Mohamed, F. A. (2011). Effect of initial microstructure on the processing of titanium using equal channel angular pressing. *Mater. Sci. Eng. A* 528 (28), 8179–8186. doi:10.1016/j.msea.2011.07.032

Dobatkin, S. V., Rokhlin, L. L., Lukyanova, E. A., Yu Murashkin, M., Dobatkina, T. V., and Yu Tabachkova, N. (2016). Structure and mechanical properties of the Mg-Y-Gd-Zr alloy after high pressure torsion. *Mater. Sci. Eng. A* 667, 217–223. doi:10.1016/j.msea.2016.05.003

Dong, B. B., Che, X., Zhang, Z. M., Yu, J. M., and Meng, M. (2021). Microstructure evolution and microhardness of Mg-13Gd-4Y-2Zn-0.5Zr alloy via pre-solution and multi-directional forging (MDF) process. *J. Alloys Compd.* 853, 157066. doi:10.1016/j.jallcom.2020.157066

Edalati, K., Fujioka, T., and Horita, Z. (2008). Microstructure and mechanical properties of pure Cu processed by high-pressure torsion. *Mater. Sci. Eng. A* 497 (1-2), 168–173. doi:10.1016/j.msea.2008.06.039

Edalati, K., Horita, Z., and Mine, Y. (2010). High-pressure torsion of hafnium. *Mater. Sci. Eng. A* 527 (7-8), 2136–2141. doi:10.1016/j.msea.2009.11.060

Edalati, K., and Horita, Z. (2010). Universal plot for hardness variation in pure metals processed by high-pressure torsion. *Mat. Trans.* 51 (5), 1051–1054. doi:10.2320/matertrans.m2009431

Edalati, K., Iwaoka, H., Toh, S., Sasaki, K., and Horita, Z. (2013). Application of high-pressure torsion to WC–Co ceramic-based composites for improvement of consolidation, microstructure and hardness. *Mat. Trans.* 54, 1540–1548. doi:10.2320/matertrans.mh201318

Edalati, K., Matsubara, E., and Horita, Z. (2009a). Processing Pure Ti by High-pressure torsion in wide ranges of pressures and strain. *Metall. Mat. Trans. A* 40, 2079–2086. doi:10.1007/s11661-009-9890-5

Edalati, K., Ito, K., Suehiro, K., and Horita, Z. (2009b). Softening of high purity aluminum and copper processed by high pressure torsion. *Int. J. Mater. Res.* 100, 1668–1673. doi:10.3139/146.110231

Edalati, K., Miresmaeili, R., Horita, Z., Kanayama, H., and Pippan, R. (2011). Significance of temperature increase in processing by high-pressure torsion. *Mater. Sci. Eng. A* 528 (24), 7301–7305. doi:10.1016/j.msea.2011.06.031

Estrin, Y., and Vinogradov, A. (2013). Extreme grain refinement by severe plastic deformation: A wealth of challenging science. *Acta Mat.* 61, 782–817. doi:10.1016/j.actamat.2012.10.038

Figueiredo, R. B., Pereira, P. H. R., and Langdon, T. G. (2020). Effect of numbers of turns of high-pressure torsion on the development of exceptional ductility in pure magnesium. *Adv. Eng. Mat.* 22 (1), 1900565. doi:10.1002/adem.201900565

Figueiredo, R. B., Sabbaghianrad, S., Giwa, A., Greer, J. R., and Langdon, T. G. (2017). Evidence for exceptional low temperature ductility in polycrystalline magnesium processed by severe plastic deformation. *Acta Mat.* 122, 322–331. doi:10.1016/j.actamat.2016.09.054

Fu, P. H., Peng, L. M., Jiang, H. Y., Ding, W. J., and Zhai, C. Q. (2014). Tensile properties of high strength cast Mg alloys at room temperature: A review. *China Foundry* 11 (4), 277–286.

Furukawa, M., Iwahashi, Y., Horita, Z., Nemoto, M., and Langdon, T. G. (1998). The shearing characteristics associated with equal-channel angular pressing. *Mater. Sci. Eng. A* 257, 328–332. doi:10.1016/s0921-5093(98)00750-3

Gao, J. H., Guan, S. K., Ren, Z. W., Sun, Y. F., Zhu, S. J., and Wang, B. (2011). Homogeneous corrosion of high pressure torsion treated Mg-Zn-Ca alloy in simulated body fluid. *Mat. Lett.* 65, 691–693. doi:10.1016/j.matlet.2010.11.015

Gleiter, H. (1989). Nanocrystalline materials. *Prog. Mat. Sci.* 33, 223–315. doi:10.1016/0079-6425(89)90001-7

Gleiter, H. (2000). Nanostructured materials: Basic concepts and microstructure. *Acta Mat.* 48, 1–29. doi:10.1016/s1359-6454(99)00285-2

Gu, G. L., Ke, X. N., Hu, F. P., Zhao, S. J., Wei, G. B., Yang, Y., et al. (2022). Fine-grained Mg-1Mn-0.5Al-0.5Ca-0.5Zn alloy with high strength and good ductility fabricated by conventional extrusion. *Trans. Nonferrous Metals Soc. China* 32 (2), 483–492. doi:10.1016/s1003-6326(22)65809-6

Gu, J., Yang, X. H., Ni, S., and Song, W. (2018). Structural and hardness evolution of pure magnesium subjected to high pressure torsion. *Rare Metal Mater. Eng.* 47 (5), 1347–1351. doi:10.1016/s1875-5372(18)30133-4

Gunderov, D., Prokoshkin, S., Churakova, A., Sheremetyev, V., and Ramazanov, I. (2021). Effect of HPT and accumulative HPT on structure formation and microhardness of the novel Ti18Zr15Nb alloy. *Mat. Lett.* 283, 128819. doi:10.1016/j.matlet.2020.128819

Hanna, A., Azzeddine, H., Huang, Y., Bradai, D., Cabrera, J. M., and Langdon, T. G. (2019b). An investigation of the thermal stability of an Mg-Dy alloy after processing by high-pressure torsion. *Mat. Charact.* 151, 519–529. doi:10.1016/j.matchar.2019.03.040

Hanna, A., Azzeddine, H., Lachhab, R., Baudin, T., Helbert, A. L., Brisset, F., et al. (2019a). Evaluating the textural and mechanical properties of an Mg-Dy alloy processed by high-pressure torsion. *J. Alloys Compd.* 778, 61–71. doi:10.1016/j.jallcom.2018.11.109

Harai, Y., Ito, Y., and Horita, Z. (2008a). High-pressure torsion using ring specimens. *Scr. Mat.* 58 (6), 469–472. doi:10.1016/j.scriptamat.2007.10.037

Harai, Y., Kai, M., Kaneko, K., Horita, Z., and Langdon, T. G. (2008b). Microstructural and mechanical characteristics of AZ61 magnesium alloy processed by high-pressure torsion. *Mat. Trans.* 49 (1), 76–83. doi:10.2320/matertrans.me200718

Heydarinia, A., Mohri, M., Asghari-Rad, P., Kim, H. S., and Nili-ahmadabadi, M. (2022). Free volume formation and the high strength of pure Mg after room temperature core-sheath ECAP passes. *J. Mat. Res. Technol.* 18, 147–158. doi:10.1016/j.jmrt.2022.02.061

Hohenwarter, A. (2015). Incremental high pressure torsion as a novel severe plastic deformation process: Processing features and application to copper. *Mater. Sci. Eng. A* 626, 80–85. doi:10.1016/j.msea.2014.12.041

Hohenwarter, A., and Pippan, R. (2011). Fracture toughness evaluation of ultrafine-grained nickel. *Scr. Mat.* 64 (10), 982–985. doi:10.1016/j.scriptamat.2011.02.007

Hohenwarter, A., and Pippan, R. (2018). Introduction of planar high pressure torsion (P-HPT) for fabrication of nanostructured sheets. *Adv. Eng. Mat.* 20 (7), 1800050. doi:10.1002/adem.201800050

Hosseini, S. A., and Manesh, H. D. (2009). High-strength, high-conductivity ultra-fine grains commercial pure copper produced by ARB process. *Mat. Des.* 30 (8), 2911–2918. doi:10.1016/j.matdes.2009.01.012

Huang, X. X. (2007). Characterization of nanostructured metals produced by plastic deformation. *J. Mat. Sci.* 42 (5), 1577–1583. doi:10.1007/s10853-006-0988-5

Huang, Y., Figueiredo, R. B., Baudin, T., Brisset, F., and Langdon, T. G. (2012). Evolution of strength and homogeneity in a magnesium AZ31 alloy processed by high-pressure torsion at different temperatures. *Adv. Eng. Mat.* 14 (11), 1018–1026. doi:10.1002/adem.201200016

Huang, Y., Figueiredo, R. B., Baudin, T., Helbert, A. L., Brisset, F., and Langdon, T. G. (2013). Microstructure and texture evolution in a magnesium alloy during processing by high pressure torsion. *Mat. Res.* 16 (3), 577–585. doi:10.1590/s1516-14392013005000025

Huang, Y., Kawasaki, M., Al-Zubaydi, A., and Langdon, T. G. (2014). Effect of anvil roughness on the flow patterns and hardness development in high-pressure torsion. *J. Mat. Sci.* 49, 6517–6528. doi:10.1007/s10853-014-8203-6

Iwahashi, Y., Horita, Z., Nemoto, M., and Langdon, T. G. (1998). Factors influencing the equilibrium grain size in equal-channel angular pressing: Role of Mg additions to aluminum. *Metall. Mat. Trans. A* 29, 2503–2510. doi:10.1007/s11661-998-0222-y

Jahedi, M., Beyerlein, I. J., Paydar, M. H., Zheng, S. J., Xiong, T., and Knezevic, M. (2017). Effects of pressure and number of turns on microstructural homogeneity developed in high-pressure double torsion. *Metall. Mat. Trans. A* 48A (3), 1249–1263. doi:10.1007/s11661-016-3923-7

Jahedi, M., Paydar, M. H., Zheng, S., Beyerlein, I. J., and Knezevic, M. (2014). Texture evolution and enhanced grain refinement under high-pressure-double-torsion. *Mater. Sci. Eng. A* 611, 29–36. doi:10.1016/j.msea.2014.05.081

Ji, H., Wu, G. H., Liu, W. C., Sun, J. W., and Ding, W. J. (2021). Role of extrusion temperature on the microstructure evolution and tensile properties of an ultralight Mg-Li-Zn-Er alloy. *J. Alloys Compd.* 876, 160181. doi:10.1016/j.jallcom.2021.160181

Jia, J. J., Meng, M., Zhang, Z. M., Yang, X., Lei, G. X., and Zhang, H. L. (2022). Effect of deep cryogenic treatment on the microstructure and tensile property of Mg-9Gd-4Y-2Zn-0.5Zr alloy. *J. Mat. Res. Technol.* 16, 74–87. doi:10.1016/j.jmrt.2021.11.137

Jung, I. H., Sanjari, M., Kim, J., and Yue, S. (2015). Role of RE in the deformation and recrystallization of Mg alloy and a new alloy design concept for Mg–RE alloys. *Scr. Mat.* 102, 1–6. doi:10.1016/j.scriptamat.2014.12.010

Kapoor, R., Kumar, N., Mishra, R. S., Huskamp, C. S., and Sankaran, K. K. (2010). Influence of fraction of high angle boundaries on the mechanical behavior of an ultrafine grained Al–Mg alloy. *Mater. Sci. Eng. A* 527, 5246–5254. doi:10.1016/j.msea.2010.04.086

Kasaeian-Naeini, M., Sedighi, M., and Hashemi, R. (2021). Severe plastic deformation (SPD) of biodegradable magnesium alloys and composites: A review of developments and prospects. *J. Magnes. Alloy* 10, 938–955. doi:10.1016/j.jma.2021.11.006

Kawasaki, M., Alhajeri, S. N., Xu, C., and Langdon, T. G. (2011). The development of hardness homogeneity in pure aluminum and aluminum alloy disks processed by high-pressure torsion. *Mater. Sci. Eng. A* 529, 345–351. doi:10.1016/j.msea.2011.09.039

Kawasaki, M., Figueiredo, R. B., Huang, Y., and Langdon, T. G. (2014b). Interpretation of hardness evolution in metals processed by high-pressure torsion. *J. Mat. Sci.* 49, 6586–6596. doi:10.1007/s10853-014-8262-8

Kawasaki, M., Lee, H. J., Ahn, B., Zhilyaev, A. P., and Langdon, T. G. (2014a). Evolution of hardness in ultrafine-grained metals processed by high-pressure torsion. *J. Mat. Res. Technol.* 3 (4), 311–318. doi:10.1016/j.jmrt.2014.06.002

Khaleghi, A. A., Akbaripanah, F., Sabbaghian, M., Máthis, K., Minárik, P., Veselý, J., et al. (2021). Influence of high-pressure torsion on microstructure, hardness and shear strength of AM60 magnesium alloy. *Mater. Sci. Eng. A* 799, 140158. doi:10.1016/j.msea.2020.140158

Khereddine, A. Y., Larbi, F. H., Azzeddine, H., Baudin, T., Brisset, F., Helbert, A. L., et al. (2013). Microstructures and textures of a Cu-Ni-Si alloy processed by high-pressure torsion. *J. Alloys Compd.* 574, 361–367. doi:10.1016/j.jallcom.2013.05.051

Kim, W. J., and Jeong, H. T. (2005). Grain-size strengthening in equal-channel-angular-pressing processed AZ31 Mg alloys with a constant texture. *Mat. Trans.* 46, 251–258. doi:10.2320/matertrans.46.251

Kloden, B., Rabacki, E., Oertel, C. G., and Skrozki, W. (2007). Grain refinement and texture formation in torsion deformed NiAl. *Int. J. Mater. Res.* 98 (4), 276–282. doi:10.3139/146.101471

Klu, E. E., Song, D., Li, C., Wang, G. W., Gao, B., Ma, A. B., et al. (2022). Achieving ultra-fine grains and high strength of Mg-9Li alloy via room-temperature ECAP and post rolling. *Mater. Sci. Eng. A* 833, 142371. doi:10.1016/j.msea.2021.142371

Klu, E. E., Song, D., Li, C., Wang, G., Zhou, Z., Gao, B., et al. (2019). Development of a high strength Mg-9Li alloy via multi-pass ECAP and post-rolling. *Metals* 9, 1008. doi:10.3390/met9091008

Kocich, R., Kunčická, L., Král, P., and Lowe, T. C. (2016). Texture, deformation twinning and hardening in a newly developed Mg-Dy-Al-Zn-Zr alloy processed with high pressure torsion. *Mat. Des.* 90, 1092–1099. doi:10.1016/j.matdes.2015.11.062

Kong, Y. P., Pu, Q. Q., Jia, Z. H., Liu, M. P., Roven, H. J., Jia, J. Q., et al. (2020). Microstructure and property evolution of Al-0.4Fe-0.15Zr-0.25Er alloy processed by high pressure torsion. *J. Alloys Compd.* 824, 153949. doi:10.1016/j.jallcom.2020.153949

Korneva, A. (2015). Microstructural changes in Cu-5.8 at.% in alloy caused by high pressure torsion. *Int. J. Mater. Res.* 106 (7), 810–812. doi:10.3139/146.111199

Kulyasova, O. B., Islamgaliev, R. K., Zhao, Y. H., and Valie, R. Z. (2015). Enhancement of the mechanical properties of an Mg-Zn-Ca alloy using high-pressure torsion. *Adv. Eng. Mat.* 17 (12), 1738–1741. doi:10.1002/adem.201500176

Langdon, T. G. (2015). Strengthening and weakening in the processing of ultrafine-grained metals. *km.* 53 (4), 213–219. doi:10.4149/km_2015_4_213

Lee, H. J., Han, J. K., Janakiraman, S., Ahn, B., Kawasaki, M., and Langdon, T. G. (2016). Significance of grain refinement on microstructure and mechanical properties of an Al-3% Mg alloy processed by high-pressure torsion. *J. Alloys Compd.* 686, 998–1007. doi:10.1016/j.jallcom.2016.06.194

Lee, H. J., Lee, S. K., Jung, K. H., Lee, G. A., Ahn, B., Lawasaki, M., et al. (2015). Evolution in hardness and texture of a ZK60A magnesium alloy processed by high-pressure torsion. *Mater. Sci. Eng. A* 630, 90–98. doi:10.1016/j.msea.2015.02.011

Lei, W. W., Liang, W., Wang, H. X., and Guo, H. W. (2017). Evolution of texture and mechanical properties of pure Mg processed by ECAP at room temperature. *JOM* 69 (11), 2297–2301. doi:10.1007/s11837-017-2497-1

Leiva, D. R., Jorge, A. M., Ishikawa, T. T., Huot, J., Fruchart, D., Miraglia, S., et al. (2010). Nanoscale grain refinement and H-sorption properties of MgH_2 processed bu high-pressure torsion and other mechanical routes. *Adv. Eng. Mat.* 12, 786–792. doi:10.1002/adem.201000030

Li, B., Teng, B. G., and Wang, E. D. (2019). Effects of accumulative rolling reduction on the microstructure characteristic and mechanical properties of Mg-Gd-Y-Zn-Zr sheets processed by hot rolling. *Mater. Sci. Eng. A* 765, 138317. doi:10.1016/j.msea.2019.138317

Li, J. W., Xu, J., Langdon, T. G., Shan, D., and Guo, B. (2016). Microstructural evolution and micro-compression in high-purity copper processed by high-pressure torsion. *Adv. Eng. Mat.* 18 (2), 241–250. doi:10.1002/adem.201500488

Li, W. T., Liu, X., Zheng, Y. F., Wang, W. H., Qiao, W., Yeung, K. W. K., et al. (2020). *In vitro* and *in vivo* studies on ultrafine-grained biodegradable pure Mg, Mg–Ca alloy and Mg–Sr alloy processed by high-pressure torsion. *Biomater. Sci.* 8 (18), 5071–5087. doi:10.1039/d0bm00805b

Li, Y. H., Li, K., Yin, W. L., and Dai, J. (2022). Microstructure and friction and wear behavior of rapidly solidified Mg-Si-RE(Ce, La) magnesium alloys. *Rare Metal. Mat. Eng.* 51 (1), 266–272.

Li, Y. S., Wang, J. H., and Xu, R. (2020). The microstructure and mechanical properties of nanocrystalline Mg-Zn-Y alloy achieved by a combination of aging and high pressure torsion. *Vacuum* 178, 109396. doi:10.1016/j.vacuum.2020.109396

Liu, B. Y., Liu, F., Yang, N., Zhai, X. B., Zhang, F., Yang, Y., et al. (2019). Large plasticity in magnesium mediated by pyramidal dislocations. *Science* 365 (6448), 73–75. doi:10.1126/science.aaw2843

Liu, M. P., Roven, H. J., YuMurashkin, M., Valiev, R. Z., Kilmametov, A., Zhang, Z., et al. (2013). Structure and mechanical properties of nanostructured Al-Mg alloys processed by severe plastic deformation. *J. Mat. Sci.* 48, 4681–4688. doi:10.1007/s10853-012-7133-4

Liu, W. H., Liu, X., Tang, C. P., Yao, W., Xiao, Y., and Liu, X. H. (2018). Microstructure and texture evolution in LZ91 magnesium alloy during cold rolling. *J. Magnesium Alloys* 6 (1), 77–82. doi:10.1016/j.jma.2017.12.002

Liu, X. H., Li, Y. S., Man, Y., Wang, J. H., and Xu, R. (2020). Precipitation and recrystallization of HPT-processed Mg-Sm-Ca alloy at low temperatures. *Mat. Lett.* 277, 128252. doi:10.1016/j.matlet.2020.128252

Liu, X. H., and Xu, R. (2022). Microstructure evolution and thermal stability of Mg-Sm-Ca alloy processed by high-pressure torsion. *J. Mat. Eng. Perform.* 31 (4), 2644–2652. doi:10.1007/s11665-021-06433-5

Lu, F. M., Ma, A. B., Jiang, J. H., Chen, J., Song, D., Yuan, Y. C., et al. (2015). Enhanced mechanical properties and rolling formability of fine-grained Mg-Gd-Zn-Zr alloy produced by equal-channel angular pressing. *J. Alloys Compd.* 643, 28–33. doi:10.1016/j.jallcom.2015.04.118

Lukyanova, E. A., Martynenko, N. S., Shakhova, I., Belyakov, A. N., Rokhlin, L. L., Dobatkin, S. V., et al. (2016). Strengthening of age-hardenable WE43 magnesium alloy processed by high pressure torsion. *Mat. Lett.* 170, 5–9. doi:10.1016/j.matlet.2016.01.106

Ma, X., Zha, M., Wang, S. Q., Wang, Y., Jia, H. L., Gao, D., et al. (2022). A rolled Mg-8Al-0.5Zn-0.8Ce alloy with high strength-ductility synergy via engineering high-density low angle boundaries. *J. Magnes. Alloy*. doi:10.1016/j.jma.2021.12.008

Mansoor, A., Du, W. B., Yu, Z. J., Liu, K., Ding, N., Fu, J. J., et al. (2022). Improved mechanical performance of double-pass extruded Mg-Gd-Er-Zr alloys with various rare Earth contents. *Mater. Sci. Eng. A* 840, 142922. doi:10.1016/j.msea.2022.142922

Matsunoshita, H., Edalati, K., Furui, M., and Horita, Z. (2015). Ultrafine-grained magnesium-lithium alloy processed by high-pressure torsion: Low-temperature superplasticity and potential for hydroforming. *Mater. Sci. Eng. A* 640, 443–448. doi:10.1016/j.msea.2015.05.103

Medvedev, A. E., Murashkin, M. Y., Enikeev, N. A., Valiev, R. Z., Hodgson, P. D., and Lapovok, R. (2018). Optimization of strength-electrical conductivity properties in Al-2Fe alloy by severe plastic deformation and heat treatment. *Adv. Eng. Mat.* 20 (3), 1700867. doi:10.1002/adem.201700867

Meng, F. Q., Rosalie, J. M., Singh, A., Somekawa, H., and Tsuchiya, K. (2014). Ultrafine grain formation in Mg-Zn alloy by *in situ* precipitation during high-pressure torsion. *Scr. Mat.* 78-79, 57–60. doi:10.1016/j.scriptamat.2014.01.036

Meng, F. Q., Rosalie, J. M., Singh, A., and Tsuchiya, K. (2015). Precipitation behavior of an ultra-fine grained Mg-Zn alloy processed by high-pressure torsion. *Mater. Sci. Eng. A* 644, 386–391. doi:10.1016/j.msea.2015.07.086

Meng, S. J., Yu, H., Fan, S. D., Li, Q. Z., Park, S. H., Suh, J. S., et al. (2019). Recent progress and development in extrusion of rare earth free Mg alloys: A review. *Acta Metall. Sin.* 32 (2), 145–168. doi:10.1007/s40195-018-00871-2

Mine, Y., Tachibana, K., and Horita, Z. (2011). Effect of hydrogen on tensile properties of ultrafine-grained type 310S austenitic stainless steel processed by high-pressure torsion. *Metall. Mat. Trans. A* 42, 1619–1629. doi:10.1007/s11661-010-0558-y

Miura, H., Maruoka, T., Yang, X., and Jonas, J. J. (2012). Microstructure and mechanical properties of multi-directionally forged Mg-Al-Zn alloy. *Scr. Mat.* 66, 49–51. doi:10.1016/j.scriptamat.2011.10.005

Miura, H., Yu, G., and Yang, X. (2011). Multi-directional forging of AZ61Mg alloy under decreasing temperature conditions and improvement of its mechanical properties. *Mater. Sci. Eng. A* 528, 6981–6992. doi:10.1016/j.msea.2011.05.050

Mulyukov, K. Y., Korznikova, G. G., and Valiev, R. Z. (1991). Microstructure and magnetic properties of submicron grained cobalt after large plastic deformation and their variation during annealing. *Phys. Stat. Sol.* 125, 609–614. doi:10.1002/pssa.2211250222

Munnoz-Morris, M. A., Oca, C. G., and Morris, D. G. (2003). Mechanical behaviour of dilute Al-Mg alloy processed by equal channel angular pressing. *Scr. Mat.* 48, 213–218. doi:10.1016/s1359-6462(02)00501-8

Nie, F. L., Zheng, Y. F., Cheng, Y., Wei, S. C., and Valiev, R. Z. (2010). *In vitro* corrosion and cytotoxicity on microcrystalline, nanocrystalline and amorphous NiTi alloy fabricated by high pressure torsion. *Mat. Lett.* 64, 983–986. doi:10.1016/j.matlet.2010.01.081

Nie, K. B., Wang, X. J., Hu, X. S., Wu, Y. W., Deng, K. K., Wu, K., et al. (2011). Effect of multidirectional forging on microstructures and tensile properties of a particulate reinforced magnesium matrix composite. *Mater. Sci. Eng. A* 528 (24), 7133–7139. doi:10.1016/j.msea.2011.06.016

Oberdorfer, B., Lorenzoni, B., Unger, K., Sprengel, W., Zehetbauer, M., Pippan, R., et al. (2010). Absolute concentration of free volume-type defects in ultra-fine-grained Fe prepared by high-pressure torsion. *Scr. Mat.* 63, 452–455. doi:10.1016/j.scriptamat.2010.05.007

Öğüt, S., Kaya, H., and Kentli, A. (2022). Comparison of the effect of equal channel angular pressing, expansion equal channel angular pressing, and hybrid equal channel angular pressing on mechanical properties of AZ31 Mg alloy. *J. Mat. Eng. Perform.* 31, 3341–3353. doi:10.1007/s11665-021-06430-8

Peng, Q. M., Wu, Y. M., Fang, D. Q., Meng, J., and Wang, L. M. (2007). Microstructures and properties of Mg-7Gd alloy containing Y. *J. Alloys Compd.* 430 (1-2), 252–256. doi:10.1016/j.jallcom.2006.05.004

Peng, X., Liu, W. C., and Wu, G. H. (2022). Strengthening-toughening methods and mechanisms of Mg-Li alloy: A review. *Rare Met.* 41 (4), 1176–1188. doi:10.1007/s12598-021-01874-2

Perez-Prado, M. T., Gimazov, A. A., Ruano, O. A., Kassner, M. E., and Zhilyaev, A. P. (2008). Bulk nanocrystalline ω-Zr by high-pressure torsion. *Scr. Mat.* 58, 219–222. doi:10.1016/j.scriptamat.2007.09.043

Popov, V. V., Popova, E. N., Stolbovskii, A. V., Pilyugin, V. P., and Arkhipova, N. K. (2012a). Nanostructurization of Nb by high-pressure torsion in liquid nitrogen and the thermal stability of the structure obtained. *Phys. Met. Metallogr.* 113, 295–301. doi:10.1134/s0031918x1203009x

Popov, V. V., Popova, E. N., and Stolbovskiy, A. V. (2012b). Nanostructuring Nb by various techniques of severe plastic deformation. *Mater. Sci. Eng. A* 539, 22–29. doi:10.1016/j.msea.2011.12.082

Qiao, X. G., Zhao, Y. W., Gan, W. M., Chen, Y., Zheng, M. Y., Wu, K., et al. (2014). Hardening mechanism of commercially pure Mg processed by high pressure torsion at room temperature. *Mater. Sci. Eng. A* 619, 95–106. doi:10.1016/j.msea.2014.09.068

Qu, X., An, X. H., Yang, H. J., Huang, C. X., Yang, G., Zang, Q. S., et al. (2009). Microstructural evolution and mechanical properties of Cu-Al alloys subjected to equal channel angular pressing. *Acta Mat.* 57 (5), 1586–1601. doi:10.1016/j.actamat.2008.12.002

Ren, K. X., Zhang, K. X., Zhang, Y., Ju, J., Yan, K., Jiang, J. H., et al. (2021). Effect of ECAP temperature on formation of triple heterogeneous microstructure and mechanical properties of Zn-1Cu alloy. *Mater. Sci. Eng. A* 826, 141990. doi:10.1016/j.msea.2021.141990

Roghani, H., Borhari, E., Shams, S. A. A., Lee, C. S., and Jafarian, H. R. (2022). Effect of concurrent accumulative roll bonding (ARB) process and various heat treatment on the microstructure, texture and mechanical properties of AA1050 sheets. *J. Mat. Res. Technol.* 18, 1295–1306. doi:10.1016/j.jmrt.2022.03.001

Saito, Y., Tsuji, N., Utsunomiya, H., Sakai, T., and Hong, R. G. (1998). Ultra-fine grained bulk aluminum produced by accumulative roll-bonding (ARB) process. *Scr. Mat.* 39, 1221–1227. doi:10.1016/s1359-6462(98)00302-9

Sergueeva, A. V., Stolyarov, V. V., Valiev, R. Z., and Mukherjee, A. K. (2001). Advanced mechanical properties of pure titanium with ultrafine grained structure. *Scr. Mat.* 45, 747–752. doi:10.1016/s1359-6462(01)01089-2

Shabashov, V. A. (1995). Polymorphism of Fe-Ni and Fe-Mn nanostructured alloys subjected to pressure shear. *Nanostructured Mater.* 6, 711–714. doi:10.1016/0965-9773(95)00157-3

Shahmir, H., and Langdon, T. G. (2016). Characteristics of the allotropic phase transformation in titanium processed by high-pressure torsion using different rotation speeds. *Mater. Sci. Eng. A* 667, 293–299. doi:10.1016/j.msea.2016.05.001

Shao, L., Zhang, C., Li, C. Y., Tang, A. T., Liu, J. G., Yu, Z. W., et al. (2022). Mechanistic study of Mg-Mn-Al extrusion alloy with superior ductility and high strength. *Mat. Charact.* 183, 111651. doi:10.1016/j.matchar.2021.111651

Silva, C. L. P., Tristão, I. C., Sabbaghianrad, S., Torbati-Sarraf, S. A., Figueiredo, R. B., and Langdon, T. G. (2017). Microstructure and hardness evolution in magnesium processed by HPT. *Mat. Res.* 20 (S1), 2–7. doi:10.1590/1980-5373-mr-2017-0223

Sitdikov, O., Sakai, T., Miura, H., and Hama, C. (2009). Temperature effect on fine-grained structure formation in high-strength Al alloy 7475 during hot severe deformation. *Mater. Sci. Eng. A* 516, 180–188. doi:10.1016/j.msea.2009.03.037

Skrotzki, W., Pukenas, A., Odor, E., Joni, B., Ungar, T., Volker, B., et al. (2020). Microstructure, texture, and strength development during high-pressure torsion of CrMnFeCoNi high-entropy alloy. *Crystals* 10 (4), 336. doi:10.3390/cryst10040336

Srinivasarao, B., Zhilyaev, A. P., Gutiérrez-Urrutia, I., and Pérez-Prado, M. T. (2013). Stabilization of metastable phases in Mg-Li alloys by high-pressure torsion. *Scr. Mat.* 68 (8), 583–586. doi:10.1016/j.scriptamat.2012.12.008

Su, Q., Xu, J., Li, Y. Q., Yoon, J. I., Shan, D. B., Guo, B., et al. (2018). Microstructural evolution and mechanical properties in superlight Mg-Li alloy processed by high-pressure torsion. *Materials* 11, 598. doi:10.3390/ma11040598

Sun, W. T., Qiao, X. G., Zheng, M. Y., Xu, C., Gao, N., and Starink, M. J. (2017b). Microstructure and mechanical properties of a nanostructured Mg-8.2Gd-3.8Y-1.0Zn-0.4Zr supersaturated solid solution prepared by high pressure torsion. *Mat. Des.* 135, 366–376. doi:10.1016/j.matdes.2017.09.048

Sun, W. T., Qiao, X. G., Zheng, M. Y., Zhao, X. J., Chen, H. W., Gao, N., et al. (2018). Achieving ultra-high hardness of nanostructured Mg-8.2Gd-3.2Y-1.0Zn-0.4Zr alloy produced by a combination of high pressure torsion and ageing treatment. *Scr. Mat.* 155, 21–25. doi:10.1016/j.scriptamat.2018.06.009

Sun, W. T., Xu, C., Qiao, X. G., Zheng, M. Y., Kamado, S., Gao, N., et al. (2017a). Evolution of microstructure and mechanical properties of an as-cast Mg-8.2Gd-3.8Y-1.0Zn-0.4Zr alloy processed by high pressure torsion. *Mater. Sci. Eng. A* 700, 312–320. doi:10.1016/j.msea.2017.05.115

Suwas, S., and Soumita, M. (2019). Texture evolution in severe plastic deformation processes. *Mat. Trans.* 62 (8), 1457–1471. doi:10.2320/matertrans.mf201933

Tang, L. C., Liu, C. M., Chen, Z. Y., Ji, D. W., and Xiao, H. C. (2013). Microstructures and tensile properties of Mg-Gd-Y-Zr alloy during multidirectional forging at 773 K. *Mat. Des.* 50, 587–596. doi:10.1016/j.matdes.2013.03.054

Tang, L. L., Zhao, Y. H., Islamgaliev, R. K., Valiev, R. Z., and Zhu, Y. T. (2017). Microstructure and thermal stability of nanocrystalline Mg-Gd-Y-Zr alloy processed by high pressure torsion. *J. Alloys Compd.* 721, 577–585. doi:10.1016/j.jallcom.2017.05.164

Tighiouaret, S., Lachhab, R., Hanna, A., Azzeddine, H., Huang, Y., Baudin, T., et al. (2019). Thermal stability of an Mg-Nd alloy processed by high-pressure torsion. *Adv. Eng. Mat.* 21, 1900801. doi:10.1002/adem.201900801

Torbati-Sarraf, S. A., Sabbaghianrad, S., Figueiredo, R. B., and Langdon, T. G. (2017). Orientation imaging microscopy and microhardness in a ZK60 magnesium alloy processed by high-pressure torsion. *J. Alloys Compd.* 721, 185–193. doi:10.1016/j.jallcom.2017.04.054

Torbati-Sarraf, S. A., Sabbaghianrad, S., and Langdon, T. G. (2015). Microstructural properties, thermal stability and superplasticity of a ZK60 Mg alloy processed by high-pressure torsion. *LoM.* 5 (3), 287–293. doi:10.22226/2410-3535-2015-3-287-293

Torbati-Sarraf, S. A., Sabbaghianrad, S., and Langdon, T. G. (2018). Using post-deformation annealing to optimize the properties of a ZK60 magnesium alloy processed by high-pressure torsion. *Adv. Eng. Mat.* 20 (2), 1700703. doi:10.1002/adem.201700703

Toroghinejad, M. R., Ashrafizadeh, F., and Jamaati, R. (2013). On the use of accumulative roll bonding process to develop nanostructured aluminum alloy 5083. *Mater. Sci. Eng. A* 561, 145–151. doi:10.1016/j.msea.2012.11.010

Towle, L. C., and Riecker, R. E. (1969). Shear strength of grossly deformed solids. *Science* 163, 41–47. doi:10.1126/science.163.3862.41

Tugcu, K., Sha, G., Liao, X. Z., Trimby, P., Xia, J. H., Murashkin, M. Y., et al. (2012). Enhanced grain refinement of an Al-Mg-Si alloy by high-pressure torsion processing at 100 °C. *Mater. Sci. Eng. A* 552, 415–418. doi:10.1016/j.msea.2012.05.063

Valiev, R. Z., Alexandrov, I. V., Zhu, Y. T., and Lowe, T. C. (2002). Paradox of strength and ductility in metals processed by severe plastic deformation. *J. Mat. Res.* 17, 5–8. doi:10.1557/jmr.2002.0002

Valiev, R. Z., Estrin, Y., Horita, Z., Langdon, T. G., Zechetbauer, M. J., and Zhu, Y. T. (2006). Producing bulk ultrafine-grained materials by severe plastic deformation. *JOM* 58, 33–39. doi:10.1007/s11837-006-0213-7

Valiev, R. Z., Ivanisenko Yu, V., Rauch, E. F., and Baudelet, B. (1996). Structure and deformaton behaviour of Armco iron subjected to severe plastic deformation. *Acta Mat.* 44 (12), 4705–4712. doi:10.1016/s1359-6454(96)00156-5

Valiev, R. Z., Korznikov, A. V., and Mulyukov, N. K. (1993). Structure and properties of ultra-fine grained materials produced by severe plastic deformation. *Mater. Sci. Eng. A* 168, 141–148. doi:10.1016/0921-5093(93)90717-s

Valiev, R. Z., Krasilnikov, N. A., and Tsenev, N. K. (1991). Plastic deformation of alloys with submicron-grained structure. *Mater. Sci. Eng. A* 137, 35–40. doi:10.1016/0921-5093(91)90316-f

Valiev, R. Z., and Langdon, T. G. (2006). Principles of equal-channel angular pressing as a processing tool for grain refinement. *Prog. Mat. Sci.* 51, 881–981. doi:10.1016/j.pmatsci.2006.02.003

Valiev, R. Z., Mulyukov, R. R., and Ovchinnikov, V. V. (1990). Direction of a grain-boundary phase in submicrometre-grained iron. *Philos. Mag. Lett.* 62, 253–256. doi:10.1080/09500839008215131

Verleysen, P., and Lanjewar, H. (2020). Dynamic high pressure torsion: A novel technique for dynamic severe plastic deformation. *J. Mat. Process. Technol.* 276, 116393. doi:10.1016/j.jmatprotec.2019.116393

Verstraete, K., Helbert, A. L., Brisset, F., Benoit, A., Paillard, P., and Baudin, T. (2015). Microstructure, mechanical properties and texture of an AA6061/AA5754 composite fabricated by cross accumulative roll bonding. *Mater. Sci. Eng. A* 640, 235–242. doi:10.1016/j.msea.2015.05.106

Wadsack, R., Pippan, R., and Schedler, B. (2003). Structural refinement of chromium by severe plastic deformation. *Fusion Eng. Des.* 66-68, 265–269. doi:10.1016/s0920-3796(03)00136-4

Wang, L. F., Li, Y. Q., Zhang, H., Zhang, Z. Y., Yang, Q. S., Zhang, Q., et al. (2020). Review: Achieving enhanced plasticity of magnesium alloys below recrystallization temperature through various texture control methods. *J. Mat. Res. Technol.* 9 (6), 12604–12625. doi:10.1016/j.jmrt.2020.09.002

Wang, S. H., Ma, J. F., Yang, J. L., Zhang, W. C., Sun, Y. P., Pan, J. Q., et al. (2021). Improving the ductility of Mg-2.5Nd-0.5Zn-0.5Zr alloy by multi-pass hot rolling. *J. Mat. Res. Technol.* 14, 2124–2130. doi:10.1016/j.jmrt.2021.07.124

Wang, Y. B., Ho, J. C., Cao, Y., Liao, X. Z., Li, H. Q., Zhao, Y. H., et al. (2009). Dislocation density evolution during high pressure torsion of a nanocrystalline Ni-Fe alloy. *Appl. Phys. Lett.* 94, 091911. doi:10.1063/1.3095852

Wang, Y. N., and Huang, J. C. (2003). Texture analysis in hexagonal materials. *Mat. Chem. Phys.* 81 (1), 11–26. doi:10.1016/s0254-0584(03)00168-8

Wei, P. T., Lu, C., Tieu, K., Su, L. H., Deng, G. Y., and Huang, W. B. (2017). A study on the texture evolution mechanism of nickel single crystal deformed by high pressure torsion. *Mater. Sci. Eng. A* 684, 239–248. doi:10.1016/j.msea.2016.11.098

Wei, Q., Zhang, H. T., Schuster, B. E., Ramesh, K. T., Valiev, R. Z., Kecskes, L. J., et al. (2006). Microstructure and mechanical properties of super-strong nanocrystalline tungsten processed by high-pressure torsion. *Acta Mat.* 54 (15), 4079–4089. doi:10.1016/j.actamat.2006.05.005

Wilde, G., Ribbe, J., Reglitz, G., Wegner, M., Rosner, H., Estrin, Y., et al. (2010). Plasticity and grain boundary diffusion at small grain sizes. *Adv. Eng. Mat.* 12, 758–764. doi:10.1002/adem.200900333

Xiao, H. C., Tang, B., Liu, C. M., Gao, Y. H., Yu, S. L., and Jiang, S. N. (2015). Dynamic precipitation in a Mg-Gd-Y-Zr alloy during hot compression. *Mater. Sci. Eng. A* 645, 241–247. doi:10.1016/j.msea.2015.08.022

Xie, J. S., Zhang, J. H., You, Z. H., Liu, S. J., Guan, K., Wu, R. Z., et al. (2021). Towards developing Mg alloys with simultaneously improved strength and corrosion resistance via RE alloying. *J. Magnesium Alloys* 9 (1), 41–56. doi:10.1016/j.jma.2020.08.016

Xing, J., Yang, X., Miura, H., and Sakai, T. (2008). Mechanical properties of magnesium alloy AZ31 after severe plastic deformation. *Mat. Trans.* 49, 69–75. doi:10.2320/matertrans.me200705

Xiong, R., Kwon, H., Karthik, G. M., Gu, G. H., Asghari-Rad, P., Son, S., et al. (2021). Novel multi-metal stainless steel (316L)/high-modulus steel (Fe-TiB2) composite with enhanced specific modulus and strength using high-pressure torsion. *Mat. Lett.* 303, 130510. doi:10.1016/j.matlet.2021.130510

Xu, C., Horita, Z., and Langdon, T. G. (2007). The evolution of homogeneity in processing by high-pressure torsion. *Acta Mat.* 55 (1), 203–212. doi:10.1016/j.actamat.2006.07.029

Xu, D. K., and Han, E. H. (2013). Relationship between fatigue crack initiation and activated twins in as-extruded pure magnesium twins in as-extruded pure magnesium. *Scr. Mat.* 69 (9), 702–705. doi:10.1016/j.scriptamat.2013.08.006

Xu, J., Wang, X. W., Shirooyeh, M., Xing, G. N., Shan, D. B., Guo, B., et al. (2015). Microhardness, microstructure and tensile behavior of an AZ31 magnesium alloy processed by high-pressure torsion. *J. Mat. Sci.* 50, 7424–7436. doi:10.1007/s10853-015-9300-x

Xu, Y. Z., Li, J. Y., Qi, M. F., Guo, W. H., and Deng, Y. (2022). A newly developed Mg-Zn-Gd-Mn-Sr alloy for degradable implant applications: Influence of extrusion temperature on microstructure, mechanical properties and *in vitro* corrosion behavior. *Mat. Charact.* 188, 111867. doi:10.1016/j.matchar.2022.111867

Xue, K. M., Sun, J. H., Ji, X. H., Guo, W. W., and Li, P. (2019). Effect of high-pressure torsion on microstructure and properties of TA15Ritanium alloy. *Rare Met. Mater Eng.* 48 (4), 1189–1194.

Yan, Z. M., Li, X. B., Zheng, J., Zhang, Z. M., Wang, Q., Xu, K. H., et al. (2021). Microstructure evolution, texture and mechanical properties of a Mg-Gd-Y-Zn-Zr alloy fabricated by cyclic expansion extrusion with an asymmetrical extrusion cavity: The influence of passes and processing route. *J. Magnesium Alloys* 9 (3), 964–982. doi:10.1016/j.jma.2020.06.016

Yan, Z. M., Zhang, Z. M., Li, X. B., Xu, J., Wang, Q., Zhang, G. S., et al. (2020). A novel severe plastic deformation method and its effect on microstructure, texture and mechanical properties of Mg-Gd-Y-Zn-Zr alloy. *J. Alloys Compd.* 822, 153698. doi:10.1016/j.jallcom.2020.153698

Yang, J. L., Wang, G. F., Park, J. M., and Kim, H. S. (2019). Microstructural behavior and mechanical properties of nanocrystalline Ti-22Al-25Nb alloy processed by high-pressure torsion. *Mat. Charact.* 151, 129–136. doi:10.1016/j.matchar.2019.02.029

Yang, X. Y., Sun, Z. Y., Xing, J., Miura, H., and Sakai, T. (2008). Grain size and texture changes of magnesium alloy AZ31 during multi-directional forging. *Trans. Nonferrous Metals Soc. China* 18, S200–S204. doi:10.1016/s1003-6326(10)60202-6

Yao, Y., Huang, Z. H., Ma, H., Zhang, H., Zhang, Z. M., Xu, C. J., et al. (2019). High strength Mg-1.4Gd-1.2Y-0.4Zn sheet and its strengthening mechanisms. *Mater. Sci. Eng. A* 747, 17–26. doi:10.1016/j.msea.2019.01.055

Zhang, J. W., Starink, M. J., Gao, N., and Zhou, W. L. (2011). Effect of Mg addition on strengthening of aluminium alloys subjected to different strain paths in high pressure torsion. *Mater. Sci. Eng. A* 528, 2093–2099. doi:10.1016/j.msea.2010.11.040

Zhang, N. X., Kawasaki, M., Ding, H., and Langdon, T. G. (2021). An examination of microstructural evolution and homogeneity in a magnesium AZ80 alloy processed by high-pressure torsion. *Mater. Sci. Eng. A* 806, 140832. doi:10.1016/j.msea.2021.140832

Zhang, Y. D., Jin, S. B., Trimby, P., Liao, X. Z., Murashkin, M. Y., Valiev, R. Z., et al. (2019). Strengthening mechanisms in an ultrafine-grained Al-Zn-Mg-Cu alloy processed by high pressure torsion at different temperatures. *Mater. Sci. Eng. A* 752, 223–232. doi:10.1016/j.msea.2019.02.094

Zhao, S. S., Xu, Y. J., Geng, C. G., Lin, X. P., Tang, Q., Dong, Y., et al. (2022). High temperature mechanical properties and strain hardening mechanism of directionally solidified Mg-Gd-Y alloy. *Mater. Sci. Eng. A* 833, 142337. doi:10.1016/j.msea.2021.142337

Zhao, X., Li, S. C., Zheng, Y. S., Liu, Z. R., Chen, K., Yu, J. M., et al. (2021). The microstructure evolution, texture weakening mechanism and mechanical properties of AZ80 Mg alloy processed by repetitive upsetting-extrusion with reduced deformation temperature. *J. Alloys Compd.* 883, 160871. doi:10.1016/j.jallcom.2021.160871

Zhen, H. P., Wu, R. Z., Hou, L. G., Zhang, J. H., and Zhang, M. L. (2021). Mathematical analysis and its experimental comparisons for the accumulative roll bonding (ARB) process with different superimposed layers. *J. Magnesium Alloys* 9 (5), 1741–1752. doi:10.1016/j.jma.2020.09.025

Zheng, R. X., Bhattacharjee, T., Shibata, A., Sasaki, T., Hono, K., Joshi, M., et al. (2017). Simultaneously enhanced strength and ductility of Mg-Zn-Zr-Ca alloy with fully recrystallized ultrafine grained structures. *Scr. Mat.* 131, 1–5. doi:10.1016/j.scriptamat.2016.12.024

Zheng, Y. F., and Gu, X. N. (2011). Research activities of biomedical magnesium alloys in China. *JOM* 63 (4), 105–108. doi:10.1007/s11837-011-0049-7

Zherebtsov, S. V., Salishchev, G. A., Galeyev, R. M., Valiakhmetov, O. R., Mironov, S. Y., and Semiatin, S. L. (2004). Production of submicrocrystalline structure in large-scale Ti–6Al–4V billet by warm severe deformation processing. *Scr. Mat.* 51, 1147–1151. doi:10.1016/j.scriptamat.2004.08.018

Zhilyaev, A. P., and Langdon, T. G. (2008). Using high-pressure torsion for metal processing: Fundamentals and applications. *Prog. Mat. Sci.* 53, 893–979. doi:10.1016/j.pmatsci.2008.03.002

Zhilyaev, A. P., Lee, S., Nurislamova, G. V., Valiev, R. Z., and Langdon, T. G. (2001). Microhardness and microstructural evolution in pure nickel during high-pressure torsion. *Scr. Mat.* 44 (12), 2753–2758. doi:10.1016/s1359-6462(01)00955-1

Zhou, Y. L., An, J., Luo, D. M., Hu, W. Y., Li, Y. C., Hodgson, P., et al. (2012). Microstructures and mechanical properties of as cast Mg-Zr-Ca alloys for biomedical applications. *Mat. Technol. (N. Y. N. Y).* 27 (1), 52–54. doi:10.1179/175355511x13240279340200

Zou, Y., Zhang, L. H., Wang, H. T., Tong, X., Zhang, M. L., and Zhang, Z. W. (2016). Texture evolution and their effects on the mechanical properties of duplex Mg-Li alloy. *J. Alloys Compd.* 669, 72–78. doi:10.1016/j.jallcom.2016.01.174